NTNU
Norwegian University of
Science and Technology

Floating Production in general, and a Parameter Study of a Flexible Riser for the Goliat FPSO in specific

Andrea Reinertsen

Marine Technology
Submission date: March 2017
Supervisor: Bernt Johan Leira, IMT

Norwegian University of Science and Technology
Department of Marine Technology

Floating Production in general, and a Parameter Study of a Flexible Riser for the Goliat FPSO in specific

Andrea Reinertsen

6th March 2017

MASTER'S THESIS

NTNU
Norwegian University of
Science and Technology

Institute for Marine Technology

Supervisor: Professor Bernt Johan Leira

MASTER'S THESIS

for

ANDREA REINERTSEN

Autumn 2016

Floating Production in general, and a Parameter Study of a Flexible Riser for the Goliat FPSO in specific

Floating production systems enable production for increasing water depths and in areas with little infrastructure present. Such solutions are attractive for remote locations like the Barents Sea. The Goliat project is the first oil-producing field to start operation in the Barents Sea, and this platform is equipped with flexible risers. The dynamic response of a riser line depends on riser geometry, vessel movement, water depth and load level. The objective of the thesis work is to give an introduction to floating production systems, identify and categorise challenges connected to operation in arctic areas and to investigate and comment on how changing riser parameters will influence the riser response. This parameter study will be performed using RIFLEX.

The following aspects shall be considered in this thesis:

- The candidate shall give a description of the different types of floaters and components for a floating production system.

- Operational and maintenance challenges for arctic areas, the Barents Sea in particular, shall be identified and categorized. This includes infrastructure and environmental challenges.

- The candidate is to get acquainted with the computer program SIMA/RIFLEX, which is applied for static and dynamic response analysis of marine risers. An outline of this computer program and the corresponding theoretical basis is to be given.

- A flexible riser model for the Goliat FPSO is to be analysed by application of RIFLEX. Static and dynamic response analyses shall be performed. Parameter studies regarding riser geometry, hydrodynamic and environmental loads are to be performed for this system to the extent that time allows.

The work shall be carried out in the following steps

1) Study of floating production systems
2) Familiarisation with the Arctic Sea region
3) Software description of RIFLEX
4) Create a model of the Goliat FPSO
5) Perform the parameter study for flexible riser
6) Presentation of results
7) Discussion of limitations and simplifications
8) Conclusion and recommendations for further work

Literature studies of specific topics relevant to the thesis work may be included. The work-scope may prove to be larger than initially anticipated. Subject to approval from the supervisor, topics may be deleted from the list above or reduced in extent.

In the thesis, the candidate's personal contribution to the resolution of problems within the scope of the thesis work shall be presented. Theories and conclusions should be based on mathematical derivations and/or logic reasoning identifying the various steps in the deduction. The candidate should utilise the existing possibilities for obtaining relevant literature.

Supervisor: Professor Bernt J. Leira

Start: August 2016 Deadline: 6. March 2017

Bernt J. Leira

Preface

This thesis, finished in March 2017, is the final part of my Master's degree in Marine Technology at the Norwegian University of Science and Technology (NTNU). The main topic of this thesis is to investigate the behaviour of a flexible riser for the Goliat platform, and it is to some extent based on the project thesis from the autumn 2015. It is assumed that the reader of this report retains a basic knowledge within engineering science.

I would like to thank Professor Bernt J. Leira for being my supervisor, and Ph.D. candidate Yuna Zhao for help with utilizing RIFLEX in this thesis. Further, I would like to thank my friends and family, and particularly my brilliant parents, for support and valuable advice throughout the process. Thank you to the best siblings ever, Amalie and Aleksander, for taking care of me in very different, but equally important, ways. Finally, I want to thank my wonderful husband, Øyvind, whithout whom the completion of my degree would have been impossible.

05.03.2017
Date

Andrea Reinertsen
Andrea Reinertsen

Abstract

A floating production system (FPS) consists of a floating structure, a mooring system, anchors and risers. Such systems enable production for larger ocean depths. Risers are vertical pipes used for transportation of production fluids between the seabed and the production unit. FPS and its components are presented and discussed in this thesis. Using an FPS entails certain challenges; risers, for instance, need other properties than for fixed structures, as they will hang from the floating unit, and must be able to absorb vessel movement. FPS is also a good option in remote areas with little infrastructure, as for the Barents Sea. When operating in arctic areas, additional challenges connected to the environment must be considered. In this thesis, challenges such as darkness, low temperatures and ice issues are identified and categorised.

The Goliat field is the first operating field to start production of oil in arctic areas. At this field, a circular Floating Production, Storage and Offloading (FPSO) unit operates, and it is equipped with flexible risers. A model of this circular FPSO is modeled as a uniform cylinder with a draught of 32.2 metres. A 644 metre long steep wave flexible riser is modelled to span between the platform and the seabed in the 400 metre deep water. A parameter study is performed to investigate the influence on the riser response. The analyses are performed in RILFEX, a software utilized for static and dynamic analysis of slender marine structures. The

varying parameters are the current profile, the riser diameter and the drag coefficient.

An analysis for varying horizontal offset of the platform, relative to the riser's touch down point (TDP) on the seabed, is also performed. The platform position that results in lowest effective tension in the riser, is 250 metres away from TDP. For this case, the riser also has lowest response amplitude.

Analyses are performed for three current profiles, uniform current, linear current and no current. It is found that by increasing the current, curvature near the riser top decreases. The case where linear current is applied, the largest tension in the riser occurs. Current variation also leads to change in the vertical displacement. For the case with no current, the riser top has a larger displacement in the negative z-direction, compared to the cases when current is applied.

The next parameter subject to change is the diameter, and three cases were studied. For increasing diameter, the weight is also increased, and the additional buoyancy due to increased volume, does not even out the added weight. As a consequence, some results might be affected more by the weight change, rather than by the change of diameter. Regarding curvature and tension, the two risers with largest diameter and weight behaves similarly, compared to the smallest riser. The two largest diameters experience larger tension and have less curvature at the hangoff, which corresponds with the additional weight.

The last parameter that was studied was the drag coefficient. For variation in diameter and drag, the displacement in vertical direction is only slightly affected near the riser top. As it is the riser properties that are changed, rather than external loading, the vessel motion is not significantly affected. The vertical displacement of the riser is affected more by change of riser properties at positions further from the vessel.

Sammendrag

Flytende produksjonssystemer (FPS) består av en flytende struktur, stigerør og et forankringssystem med forankringsliner og ankere. Slike systemer muliggjør produksjon på større havdyp. I denne oppgaven blir FPS med tilhørende komponenter presentert og diskutert. Bruk av flytende produksjonssystemer fører med seg noen utfordringer, for eksempel krever stigerør andre karakteristiske egenskaper enn for bunnfaste strukturer. Stigerør brukes for å transportere oilje, gass og vann mellom havbunnen og produksjonsenheten. FPS er også en attraktiv løsning for fjerntliggende områder med lite eksisterende infrastruktur, som for eksempel i Barentshavet. Når man opererer i artiske områder, må også andre utfordringer tas i betraktning. Disse er hovedsakelig knyttet til miljø- og værmessige faktorer som mørke, lav temperatur og fare for is. Slike utfordringer er identifisert og kategorisert i denne oppgaven.

Goliat-feltet er det første til å drive oljeutvinning i Barentshavet. Dette feltet har en sirkulær FPSO (Floation Production, Storage and Offloading) som er utstyrt med fleksible stigerør. I denne oppgaven, er en modell av Goliat-plattformen modellert som en uniform sylinder med en dypgang på 32,2 meter. Et 644 meter langt fleksibelt stigerør med «steep wave»-konfigurasjon er modellert for å spenne fra flyteren til havbunnen. Havdybden er 400 meter.

En parameterstudie er gjennomfør for å undersøke påvirkningen på stigerørets re-

spons. Denne analysen er gjennomført i RIFLEX, en programvare for statisk og dynamisk analyse for slanke, marine strukturer. Parameterne som er variert i dette tilfellet er strømningsprofil, stigerørets diameter og drag-koeffisienten.

En analyse for varierende horisontal avstand mellom plattformen og stigerørets forankringspunkt på havbunnen (TDP) ble også gjennomført. Den plattformposisjonen som førte til lavest effektiv strekk i stigerøret, var 250 meter fra TDP.

I parameterstudien, ble en analyse utfør for tre ulike strømningsprofiler, uniform strøm, lineær strøm og uten strøm. For økende strømning reduseres krumingen i toppen av stigerøret. Lineær strømning gir høyere maksimal effektiv strekk enn for uniform strømning og ingen strømning. Variasjon i strømningen fører også til endring i vertikal forskyvning. For tilfellet uten strømning forskyves toppen av stigerøret dypere enn for tilfellene med strøm.

For økende diameter ble også vekten økt. Det økte volumet og tilhørende oppdrift, utjevner ikke den ekstra vekten. På grunn av dette kan vektvariasjonen ha større påvirning på resultater enn diametervariasjonen har. Når det gjelder kurvatur og strekk, har de to stigerørene med størst diameter og vekt mer liknende oppførsel, sammenliknet med det siste, minste stigerøret. De to største diameterne gir høyere strekk og lavere kurvatur i det øvre festepunktet, noe som stemmer overens med den tunge vekten.

For variasjon i diameter og drag, er forskyvningen i vertikal retning påvirket lite ved stigerørets festepunkt. Ettersom det er stigerørets egenskaper som endres, og ikke ytre krefter, vil dette ikke ha særlig påvirkning på plattformens respons. Vertikal forflytning av stigerøret er mer påvirket av endringene lenger borte fra plattformen.

Table of Contents

List of Figures

List of Tables

Nomenclature

Abbreviations

COB	Centre of Buoyancy
COG	Centre of Gravity
DDF	Deep Draught Floater
DP	Dynamic Positioning
FEM	Finite Element Method
FPSO	Floating Production, Storage and Offloading
JONSWAP	JOint North Sea WAve Project
LOA	Length Over All
MFC	Minimum Force Configration
TDP	Touch Down Point
TLP	Tension Leg Platform
TTR	Top-Tensioned Riser

Roman symbols

A_i	Internal cross-sectional area
A_o	External cross-sectional area
a_1	Fluid acceleration
B	Bredth
C_A	Added mass coefficient
C_D	Drag coefficient
C_M	Mass coefficient
C_D^T	Tangential drag coefficient
C_M^T	Tangential mass coefficient
$\bar{D}$	Draught
D	External diameter
d	Internal diameter
F	Force
H_S	Significant wave height
I_{ii}	Moment of inertia
I_{ij}	Product of inertia
K_C	Keulegan-Carpenter number
k	Roughness height
k	Wave number
L	Length
M_{Tot}	Total mass
m_i	Mass of section
p_i	Internal pressure
p_o	Externar pressure
R_e	Reynolds number
R_{ij}	Radius of gyration

$\boldsymbol{R}^D$	Damping force vector
$\boldsymbol{R}^I$	Inertia force vector
$\boldsymbol{R}^S$	Internal, structural reaction force vector
$\boldsymbol{R}^E$	External force vector
$\boldsymbol{r}$	Nodal displacement
$\dot{\boldsymbol{r}}$	Nodal velocity
$\ddot{\boldsymbol{r}}$	Nodal acceleration
$S_J(\omega)$	The JONSWAP spectra
T	Wave period
T_e	Effective tension
T_p	Peak period
T_w	Wall tension
t	Time
u	Fluid velocity
U	Current velocity
v_m	Maximum orbital velocity

Greek symbols

Δ	Non-dimensional roughness
γ	Non-dimensioning peak shape parameter
ν	Fluid kinematic viscosity
ξ	Wave profile
ξ_a	Wave amplitude
σ	Spectral width parameter
ρ	Density
ω	Circular frequency
ω_p	Circular peak frequency

Chapter 1

Introduction

1.1 Motivation

There are two main types of offshore structures, fixed and floating. For increasing water depths, utilization of fixed structures result in structural challenges and increasing cost. Floating structures are hence more common now than earlier, as the offshore industry is locating fields with increasing water depths. The floating structures are equipped with risers, the pipes through which production fluids are transported, and mooring lines. As the structure is floating, the risers will hang, and must handle floater movement.

The Goliat Field in the Barents Sea has a circular floating offshore unit, it is equipped with flexible risers. As the platform is located in the Barents Sea, it is subject to several major challenges. Due to a remote location and tough environmental conditions, development of production facilities in arctic areas requires additional consideration regardring suc challenges. Operation and maintenance require thorough planning in order to be executed in an efficient and safe manner.

1.2 Objective

It is of interest to learn about floating production systems and about the Goliat platform specifically. As the Goliat platform is located in the Barents Sea, it is useful to identify challenges connected to locating production fields in arctic areas. Obtaining the characteristic motion of the Goliat platform and how the risers connected to it will behave, are topics desirable to investigate further.

1.3 Scope and Limitations

In this thesis, floating production systems and its components will be presented and discussed. The Goliat Field will be presented, and arctic offshore challenges will be identified and categorized.

A model representing the Goliat platform will be modellen in the software GeniE, and a hydrodynamic analysis will be performed utilizing HydroD. This will be performed for a sea state for the Goliat field in the Barents Sea. The platform's characteristic motion will be found, and this will be connected to a riser, and a parameter study will be carried out in order to investigate the respons behaviour of the riser. This will be performed utilizing RIFLEX.

1.4 Outline

In Chapter 2, a general presentation of floating production systems is given. The Goliat Field is presented in Chapter 3, including an introduction to operational challenges in the Barents Sea. Chapter 4 contains a software description of the softwares utilized in this thesis, with emphasis on RIFLEX. A general description

of loading mechanisms is given in Chapter 5, and some relevant rules and recommendations from DNV are described in Chapter 6. The parameter study, and a subsequent analysis regarding horizontal offset, is presented in Chapter 7. The results and discussion are found in Chapters 8 and 9, respectively. In Chapter 10, conclusion and suggestions for further work is given.

Chapter 2

Floating Production Systems

A floating production system (FPS) consists of a floater, a mooring system and risers. A mooring system consists of mooring lines and anchors. The choice of these components depend on the environment at the location for the specific operation/production, and how the sub-systems are compatible with each other. Some FPS variants are displayed in Figure 2.1.

2.1 Floater

A common feature of the floaters used in a floating production system is that the topside contains the living quarters, necessary equipment and production facilities. The floater contributes with additional buoyancy to support this deck payload. The processing equipment aboard the floater is similar to what would be found atop a fixed production platform. The most common floater types have different qualities and characteristics, and can be moored in various ways. Typical for all of them is that they are so-called "soft" in the horizontal plane with ei-

genperiods larger than 100 seconds. The differences are connected to the vertical motions (DNV (2010c)). The floaters are discussed in Sections 2.1.1-2.1.5.

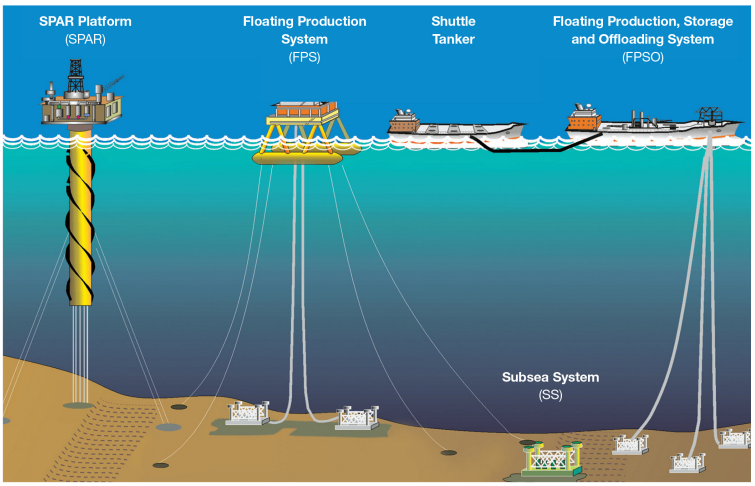

Figure 2.1: Illustation of floating production systems (API (2015))

2.1.1 Spar

The spar is recognized by the large cylindrical hull beneath the water surface and the large draught (Amdahl et al. (2011)). It is a so-called Deep Draught Floater (DDF). The vertical cylinder creates stability and carries the platform topside. The cylinder is an empty hull with ballast tanks at the very bottom and a central moonpool for a riser system. The ballast tanks are filled with material heavier than water to ensure that the location of the centre of gravity (COG) is below the centre of buoyancy (COB). Another advantage of this design, in addition to storing oil and gas, is that the deep-draught hull protects risers and other equipment from waves and current. The wave frequency motions are small, and wave and wind forces will not effect this kind of design to a large extent. Spars will hence support both subsea and dry tree installations (Rigzone (2015d)). The spar platform has a large area exposed to current forces, and this is usually the dominant environmental

load. The current forces may be increased due to larger effective drag caused by low frequency vortex induced motion (DNV (2010c)).

As mentioned, COG is located below COB, and the structure will stay upright even without mooring. Still, the platform is moored to the seabed for station keeping. Station keeping means maintaining a vessel's intenden position. Typically, DDFs experience small vertical motions, which makes it an attractive choice for instance in the Gulf of Mexico (Amdahl et al. (2011)). Heave natural period is commonly larger than the wave periods. The low vertical motion makes it possible to utilize rigid top-tensioned risers. In addition to the original Spar design, there are two common variations of this platform type; the truss spar and the cell spar. The truss version has a shorter hull, but with a truss work below. It is both cost and weight efficient (Rigzone (2015d)).

Finding the spar's centre of roll is important, as it is desirable to attach the mooring lines to points with no horizontal motion. The centre of roll, if on the body, is typically located at the bottom. In reality it could also be placed outside the body, but this is not desirable as it would cause the body to move as part of a pendulum. Centre of roll could also be non-existing (Greco (2012)).

An example of a spar platform is Aasta Hansteen. It is the world's largest spar, with a total height of nearly 200 meters, excluding the topside. Including the topside it is a total of 320 metres (Stensvold (2014)). The diameter of the deep draught hull is 50 metres . The platform is located on a gas field with the largest ocean depth on the Norwegian shelf, of about 1200 metres (Stensvold (2014)). The field lies 300 kilometers west of Bodø. An illustration of the platform can be seen in Figure 2.2.

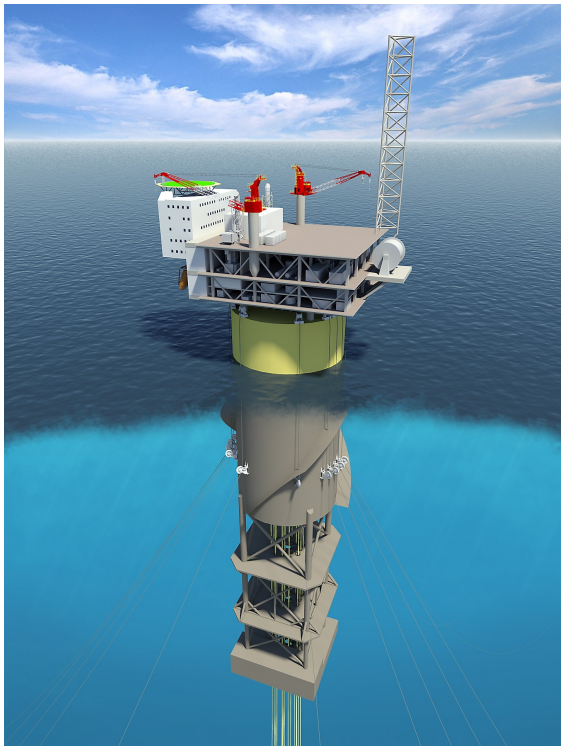

Figure 2.2: Illustration of Aasta Hansteen (Ree (2013))

2.1.2 Ship-shaped FPSO

FPSO is short for Floating Production, Storage and Offloading. An FPSO is often a ship-shaped vessel with the deck functioning as topside, and equipment is placed here. In such cases, the double hull has several large cargo tanks used for storage. Processed oil and gas is stored here until offloading. A receiving tanker carries the hydrocarbons to a reception facility.

For many FPSOs, the stern of the vessel has an offloading hose. This is a flexible connection between the FPSO and the receiving tanker. The hose is connected to the tanker's bow, and this operation is called tandem offloading. This offloading method makes FPSOs an attractive solution where there are no existing pipelines

or infrastructure to transport hydrocarbons to shore. Between offloading operations, the hose can be stored two ways; either floating in the sea or on a very large hose reel (BW Offshore (2015)). It is also a possibility to have this offloading system at the bow, or even at the side, though this is less common. Other offloading mechanisms can also be utilized. If gas is present at the field, this can be transferred to shore via pipelines (Rigzone (2015a)).

An FPSO is often turret moored, which makes it possible to rotate freely with current and wind (Amdahl et al. (2011)). This is called weathervaning and ensures best possible response behaviour to the weather. It makes operating in areas with severe weather conditions feasible (BW Offshore (2015)). There are two types of weathervaning; the passive and the active weathervaning ability. The passive kind is when the vessel naturally turns due to environmental loads, and this is not thruster assisted. Active weathervaning means using thrusters to gain desired position. This is obtained via a dynamic positioning system. The active and passive kind can also be used in combination (OTC (1995)).

The weathervaning ability causes wind forces to be more dominating than current forces. FPSOs can experience low frequency responses in the horizontal plane, and can be especially sensitive to surge excitations. For larger depths, the FPSO will be less sensitive to these excitations as mooring lines provide larger damping (DNV (2010c)).

Turret mooring enables the FPSO to disconnect from its moorings, and is hence optimal for areas that experience adverse weather, like cyclones and hurricanes. For a specific kind of turret mooring, called detachable buoy, this is a fairly quick process. The turret is commonly placed near the bow of the vessel, but can also be placed nearer to the centre or in the back. The choice depends on tanker design and field location, and safety criteria must be considered. In more calm waters,

spread mooring is typically used.

For both turret mooring and spread mooring, wind generated waves in combination with swell can be a challenge if they have different heading. Head sea in combination with beam swell is a critical condition and can cause significant roll accelerations. Thus, proper roll damping is important.

Historically, FPSOs have been operating in the North Sea, offshore Brazil, Asia Pacific, the Mediterranean Sea and offshore West Africa, and this vessel type has been in use since the 1970s (Rigzone (2015a)). The vessel can relatively easy be relocated, but it is often positioned in the same place for a longer period of time (DNV (2010c)).

Most FPSOs used today are transformed oil tankers. Another, less common, alternative is to build a vessel for this application. A main issue is whether the FPSO is to be considered an offshore structure, and to what extent maritime principles are still applicable (OTC (2001)). When FPSOs are custom built, it is often to obtaint another shape, as for instance circular FPSOs that are discussed in Section 2.1.3.

An example of a ship-shaped FPSO is Åsgard A, seen in Figure 2.3. The Åsgard field is located on the Halten bank in the Norwegian Sea, approximately 200 kilometres west of Trøndelag. It is among the largest field developments on the Norwegian shelf, and has a water depth of 240-310 metres. Åsgard A gas been in production since 1999, as the first of the three units on the field (Statoil (n.d.-c)).

Figure 2.3: Åsgard A (Oil and Gas People (2016))

2.1.3 Circular FPSO

When purpose-built units are chosen, it is for fields with large capacity and long life expectancy (McCaul (2001)). Storage capability is built into the design of the vessel. The hull design process is iterative, where the different stages are performed several times until the design converges (OTC (2001)). Advantages of this approach is for instance that it is possible to design the vessel for arctic environments, possibilities for circular design and good separation between hazardous and non-hazardous areas (Aker Engineering & Technology (2015)). As it is designed for the purpose of being an FPSO, rather than being transformed, it is more efficient and costs can be reduced.

Global loads on the hull creates minimal bending stresses, which eliminates typical wave induced fatigue loads, as well as a severe reduction of hull deflections. This will again simplify the topside design (Major (2013)).

Due to symmetry, no weathevaning is needed for a circular FPSO. Even for harsh weather conditions, the hull is subject to the same environmental loads, no matter the direction. This is an advantage as the turret, which is a complex and expensive device unit, can be excluded from the design. Without this device, circular FPSOs can be powered from shore, which is a better solution than onboard systems. The solution with no turret also enables a large number of risers connected to the platform. In particular, the circular design enables use of steel catenary risers for harsh environments, which has a lower cost, higher durability and larger flexibility (Major (2013)).

An example of a circular FPSO is the Goliat platform, illustrated in Figure 2.4, which is the platform featured in this thesis. It is located in the Barents Sea, north-west of Hammerfest. This FPSO is described further in Chapter 3, and in Section 7.1.1, the modelling of the platform is described.

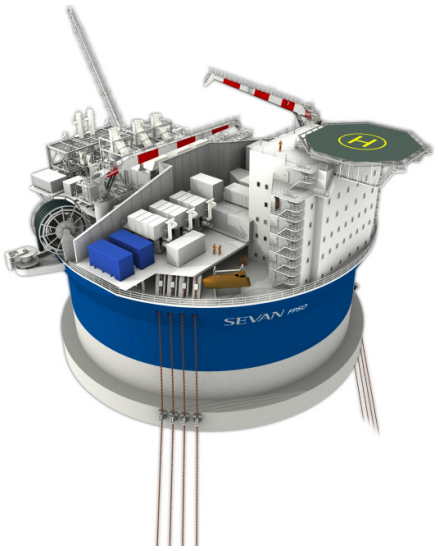

Figure 2.4: Illustration of the Goliat FPSO (SubseaIQ (2015))

2.1.4 TLP

TLP is short for Tension Leg Platform. Vertical, tensioned lines with low elasticity ensures the platform to act like a stationary structure as wave frequency forces will be directly counteracted by tendon stiffness forces, and practically no wave frequency response will occur (DNV (2010c)).

The tendons govern the vertical stiffness compared to waterplane stiffness. The motions are kept to an absolute minimum in heave, pitch and roll, as the TLP is stiff in these degrees of freedom. Horizontal movements are present as the TLP acts like a soft spring i surge, sway and yaw motions. TLPs are popular choices for stability, for instance in the Gulf of Mexico that is subject to hurricanes.

Tension leg mooring means utilizing the excess buoyancy for station keeping. The TLP platform is submerged to a larger draught than the natural one. The excess buoyancy is what ensures the constant tension in the tendons. The tension legs

can not handle axial pressure, and it is important that the tension in the legs are present at all times. The tension legs are secured to a foundation on the seabed which are kept stationary by pile anchors.

An example of a TLP is the Heidrun platform. The Heidrun field is located 50 kilometres north of the Åsgard field (Statoil (n.d.-c)) on the Halten bank in the Norwegian Sea. From the Heidrun tension leg platform, the field has produced oil and gas since 1995. Oil is mainly transported by shuttle tankers to Mongstad near Bergen, while gas is transported to shore via pipes. Since 2001, gas from Heidrun has been piped all the way to Germany, a total distance of approximately 1400 kilometres (Statoil (n.d.-a)). The water on the Heidrun field depth is around 350 metres (Holm (2016b)). An illustration of the Heidrun platform can be found in Figure 2.5.

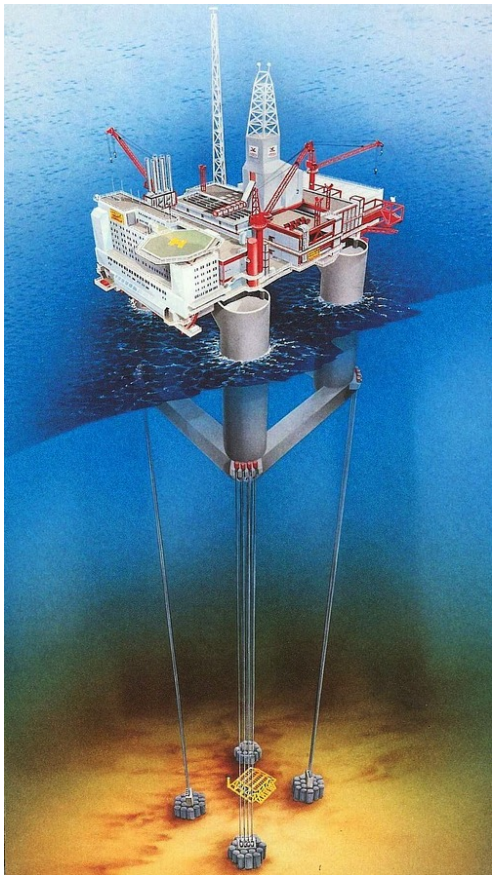

Figure 2.5: Illustration of the Heidrun TLP with its steel tethers (*Heidrun* (2015))

Higher order effects

Springing is a phenomenon due to 2^{nd} order sum-frequency effects. It is a steady-state resonant elastic motion in the vertical plane. 2^{nd} order sum-frequency effects are excited at high frequencies, and thus low periods. Due to this, structures

designed for low periods in the vertical plane, such as TLPs, may experience resonant vertical motion as result of 2^{nd} order effects. The springing effect is relevant for fatigue of the tethers.

3^{rd} and 4^{th} order effects can cause transient oscillations on this type of structures (Greco (2012)). This phenomenon is called ringing, and it is critical for the tethers' extreme tension. It is hence relevant for ultimate strength design of the tethers.

2.1.5 Semi-submersible

A semi-submersible is a column-stabilized unit. The topside is placed on supporting columns with large diameter. These are attached to pontoons submerged into the water. The pontoons can either be ring pontoons, twin pontoons or multi-footing solutions (DNV (2010c)). The semi-submersible is the most common platform type, and it is used in several kinds of operations. It is for instance commonly used in drilling operations. This floater can obtain station keeping both by mooring or by use of dynamic positioning if equipped with thrusters.

While in transit, the semi-submersible platform is not lowered to the operational draught (Rigzone (2015c)). Executing the transportation in transit draught gives an economical advantage compared to operational draught. A semi-submersible's pontoons are often ship-shaped, intended for this purpose. When desired location is reached, parts of the hull are filled with ballast water, and the vessel is lowered to the correct operational draught. The desired draught should not be changed significantly during operation, and the semi-submersible is sensitive to change in weight. This means it has low flexibility with respect to deck load and oil storage (DNV (2010c)). When the storage capacity on the platform is used, ballast

water is removed to compensate for the filling of oil tanks. The semi-submersible can also be additionally lowered until a survival draught is obtained. This is perfomed if the wave height exceeds a critical limit.

Semi-submersibles are designed for stability. The roll and pitch motions are significantly reduced by keeping the rig partially submerged. The vessel has a small waterplane area, and this causes the vertical natural period to be around 20 seconds. This is larger than the range of wave periods, except for extreme weather (DNV (2010c)). This implies low vertical displacement compared to monohull floater, but the extreme wave response can lead to motions of significant magnitude. Even though current forces have larger impact on semi-submersibles than ship shaped vessels, due to bluff body geometry, wave and wind loads will be governing in most cases. An exception is calm fields with strong current, where the current will govern the mean forces.

It is important that the air-gap below the deck is sufficiently large at all times. If this air-gap is too small in a sea state with large waves, wave impact underneath the deck can be experienced. This can be critical, and will influence global motions and local structure response (DNV (2010c)).

Figure 2.6: Snorre B semi submersible platform (Mazzetti (2015))

An example of a semi submersible is the Snorre B platform, seen in Figure 2.6. It is the second platform to start production in the Tampen area of the Norwegian North Sea. It is a PDQ floater, meaning it is an integrated production, drilling and quarters unit.

It does not have a storage unit, and the oil is piped for 45 kilometres to Statfjord B for storage and export. Gas is piped via Snorre A to continental Europe and Scotland (Statoil (n.d.-b)). The water depth on the Snorre field is approximately 350 metres (Holm (2016c)).

Higher order effects

Since the natural period of a semi-submersible is high, typically larger than 20 seconds, low-frequency effects can be important. Slow-drift and mean drift can occur due to interaction between vessel and environmental loads. It is more likely to be present in the horizontal plane for mooring systems, since the mooring lines are what causes restoring forces. This can result in natural periods up to 2 minutes.

2.2 Mooring Systems

Mooring systems control the motion and provide an exact position of the vessel. Such systems ensure resistance to environmental loads by deforming and activating reaction forces (DNV (2010c)). Functioning like a spring mechanism, restoring forces counteract the applied loading and the displacement of the floater from original position. Restoring forces are crucial in surge, sway and yaw, as these body motions are in the horizontal plane and does not have any natural restoring. The mooring system should also contribute with damping (Greco (2012)). A mooring system consists of anchors, mooring cables and connectors. An anchor is fastened at the seafloor, and is connected to the floating structure through mooring lines. In this section, mooring systems are presented.

2.2.1 Catenary Mooring

A catenary mooring system consists of free hanging lines that change shape with vessel motions. This type of mooring is defined by standard catenary formulation that are related to submerged weight of suspended lines, horizontal mooring load, line tension and line slope at fairlead (DNV (2010c)). Catenary mooring systems are often subject to dynamic effects due to transverse drag loads.

For this mooring system, the lines are significantly longer than the sea depth. These lines will be heavy if they only consist of chain and wire. Synthetic fibres are hence used if the water is sufficiently deep. This is discussed in Section 2.4. Catenary mooring is the most frequently used mooring system for shallow water (Rigzone (2015b)), but claims a lot of subsea area for large depths as the lines lie horizontally on the seabed. To reduce the seabed footprint for large depths, taut mooring can be used as an alternative, see Section 2.2.2.

2.2.2 Taut Mooring

Taut mooring is a type of spread mooring where the lines are tensioned, leading diagonally and almost straight from fairlead to the anchor on the seabed. Vertical forces are withstood directly by anchor and vessel reactions. The tensioned lines' elasticity provides the vessel's ability to move when exposed to the environmental loads.

The change in geometric shape is considerably smaller for this mooring system than for catenary systems. Dynamic effects due to transverse drag loads are hence moderate. On the other hand, synthetic ropes are frequently used as mooring cables in this system types. Synthetic ropes have complex stiffness characteristics, which may introduce dynamic effects (DNV (2010c)).

An advantage of this mooring system compared to catenary mooring, is a considerably smaller footprint as is illustrated in Figure (2.7). With this kind of mooring system, it is important to utilize anchors that can withstand both vertical and horizontal forces.

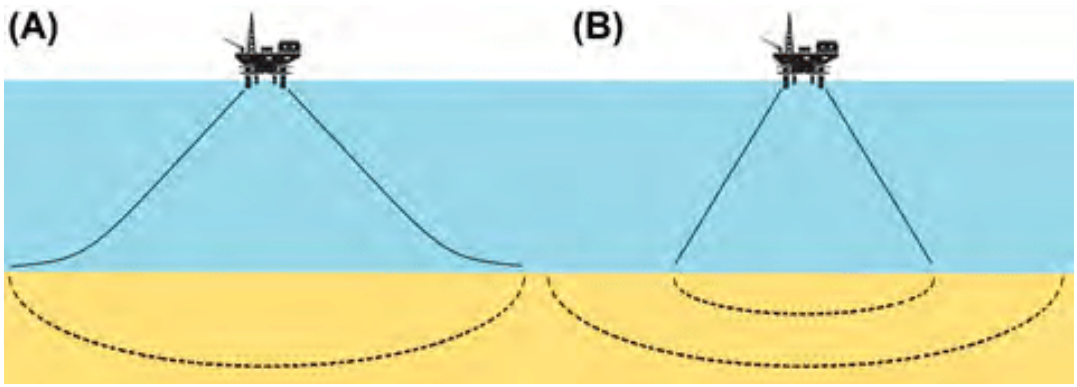

Figure 2.7: Illustration of catenary mooring (A) and taut mooring (B) (de Camargo et al. (2016))

2.2.3 Dynamc Positioning

While mooring systems keep a static position, thrusters can provide a dynamic positioning. A dynamic positioning (DP) system is defined as a computer controlled system that automatically maintains a ship's position and heading by using its own thrusters and propellers (Bjorneseth and Strand (2008)). Such a system is highly flexible considering both water depth and maneuverability, and can be used both alone and in combination with a static mooring system (Faltinsen (1990)). A DP vessel is a vessel that exclusively utilizes thrusters to maintain position and heading, i.e. without static mooring. DP systems are guided by satellites and telemetry signals from beacons on the seabed.

2.3 Anchors

The various mooring systems can be connected to different kinds of anchors that provide holding capacity. The capacity depends on the digging depth and soil friction. In this section, some of the most common anchor types are described. These are gravitational anchor, drag anchor, suction anchor, torpedo anchor and pile anchor.

2.3.1 Gravitational Anchor

Gravitational anchors keep vessels in place due to heavy weight alone. Traditionally, these consist of concrete filled with heavier material, like for instance iron ore. The concrete is easily shaped into the appropriate geometry, but does not contribute with suffieciently large weight.

2.3.2 Drag Anchor

Drag anchors are pulled along the seabed until it fastens at desired depth. It does not have the ability to withstand vertical forces. Because of this limitation, it can only be used in combination with a catenary mooring system, which has lines laying along the seabed, and only horizontal forces need to be counteracted by the anchor.

2.3.3 Suction Anchor

Suction anchors are preferable for muddy seabeds. The anchors are cylinders placed on the seabed, the air is pumped out of the cylinder, and the anchors are

dug into the soil. It is kept in place due to the friction between the anchor and the soil, negative tension in the cylinder. A critical load case for suction anchors is buckling during installation due to pressure difference outside and inside the cylinder (DNV (2010f)). This anchor type can be used in combination with gravity anchors, so that if the suction effect should fail, gravity will keep the system in correct position. This is called a skirt suction foundation. A suction anchor is less likely to lose its suction effect in muddy seabeds or clay, than for soil with particles.

2.3.4 Torpedo Anchor

The torpedo anchor is a deep penetrating anchor shaped like a torpedo. It is released from a certain heigh above the seabed, and it penetrates itself to a certain depth into the soil. This type of anchor can reach velocities up to 100 km/h during the drop and fall towards the seabed. They can weigh up to 100 tonnes and have a height of 10-15 meters (NGI (2011)). An illustration of a torpedo anchor can be seen in Figure 2.8

Figure 2.8: Torpedo anchor (*Torpedo Anchor* (2015))

2.3.5 Pile Anchor

A pile anchor is a slender unit driven far into the ground. The resistance force is dependent on the soil properties, the depth and angle of the pile and the pile

geomtry and slenderness.

2.4 Mooring Lines

The mooring lines consist of different material types. The material choices depend on the desired properties and behaviour of the lines. The three materials most frequently used for mooring line segments are chain, synthetic fibre ropes and steel wire. They can in general be used alone or in combination (DNV (2010f)). The possibilities are discussed in Sections 2.4.1-2.4.4.

2.4.1 Chain

Chain is a common choice for permanent mooring in shallow water. It is convenient to hoist onto a reel. There are different chain types for permanent mooring and temporary mooring of vessels that frequently change locations. The requirements are stricter for the permanent mooring. There are for instance several shackle types prohibited used in long-term mooring systems due to poor fatigue qualities (DNV (2010f)).

2.4.2 Steel Wire

With higher elasticity and lower weight than chain, wire is a better choice for water depths exceeding 300 meters. In the same way as for chain, this line type has different requirements for long-term mooring, compared to mobile mooring and towing. The wire needs to pass certain tests to operate as one or the other. Either way it is important that the rope is of homogeneous quality (DNV (2009)).

2.4.3 Synthetic Fibre Ropes

Synthetic fibre rope is the lightest of the three line types. It contributes with high elasticity and low self-weight. This line type is only used in combination with one or both of the two mooring line types previously described, wire and chain. The synthetic fibre line segment should be submerged at all times during the operation, and the load bearing parts of the rope should not be exposed to sunlight (DNV (2010f)). Synthetic ropes have, as mentioned in Section 2.2.2, complex stiffness characteristics, and this may induce important dynamic effects (DNV (2010c)).

2.4.4 Cable Combinations

As mentioned, cable configurations can include a combinations of the materials described. This is relevant for deeper waters. A conventional mooring line up to the length of 2000 meters can for instance consist of line segments from both chain and wire rope. For ultra-deepwater mooring, a chain and synthetic fibre rope combination can be applied, or a solution including all three line types can be utilized (Rigzone (2015b)). For this kind of mooring lines, chain is often used at the top and at the bottom. At the top, chain is convenient to hoist onto a reel, and at the bottom it contributes with weight, and it will lay steady on the seabed and prevent uplift of anchor.

2.5 Riser System

Oil, gas and produced water is transported through pipes designed for vertical transportation. These are called risers and function as the connection between floater and the subsea components. For fixed platforms, risers can be clamped to the structure's leg. When a platform is floating, it is not possible to use this method, and the risers must hence have different properties when used in a floating production system. Risers can be either rigid or flexible. These two options will be further discussed in the following sections. In general, forces working on risers are described by Morison's equation (Faltinsen (1990)). The Morison's equation is discussed in Section 5.2.

2.5.1 Compliant Riser Systems

Compliant riser configuration is designed to compensate for vessel motions by changing the geometry, without heave compensation. Such risers are also called flexible risers. The complex cross-section of flexible risers consist of several layers. There are layers with different functions, as friction layers, layers providing collapse resistance and carrying layers that withstand pressure. The carrying layers are also protecting the risers from the surrounding environment. A flexible riser can made from a combination of steel and plastic, or from steel alone.

The most critical section of a flexible riser with respect to fatigue will be the upper hang off. Here, the contact pressure conditions are dominated by internal pressure and tension. This will govern the fatigue behaviour as the largest contact pressure, and associated friction stresses, will effect the inside of the riser here (Sævik (2015)).

2.5.2 Flexible Riser Configurations

Figure 2.9 displays five common flexible riser configurations. A short description of these five follows.

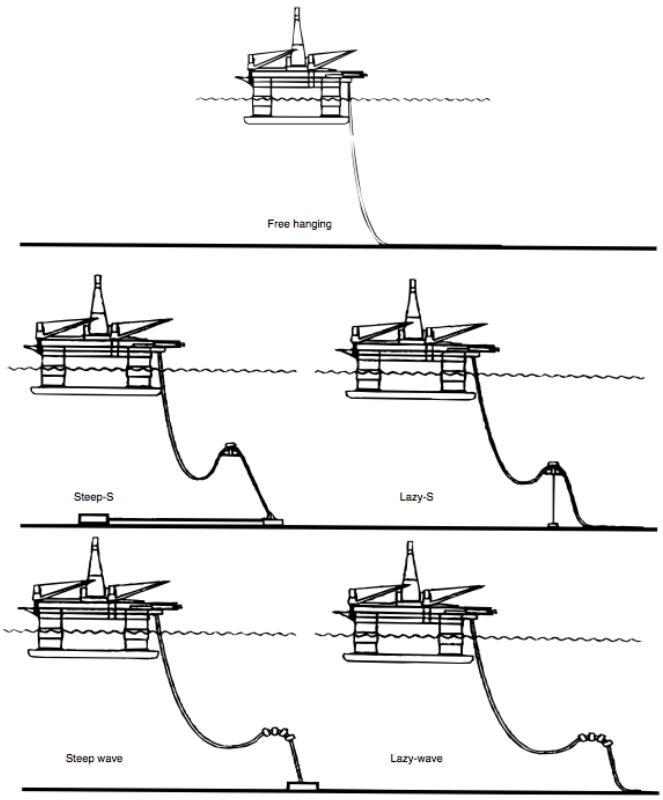

Figure 2.9: Illustation of riser configurations (API (2002))

Free Hanging Catenary

A free hanging catenary riser is not designed to handle large motions from vessels. It is a simple catenary resting on the seabed. It has limited additional length to absorb vessel motion. It is hence most suitable in calm operational fields. Large vessel motions can contribute to compression at the touch down point, which can lead to buckling. The simple design makes it an attractive solution, considering

the economical aspect.

Lazy Wave

The Lazy wave configuration is quite similar to the free hanging catenary, but this configuration has the ability to handle vessel motions due to a subsurface loop prior to the touch down point. In addition to providing with flexibility regarding motion, the buoyancy elements creating this loop also carry some of the riser weight. This reduces the static tension at the vessel connectors. A negative effect is that the buoyancy section will have a larger diameter, hence drag forces will increase and there is a risk of risers moving on the seabed without returning to initial position.

Lazy S

The only difference from Lazy wave configuration is that the Lazy S has one large buoyancy element instead of having multiple small ones. The buoyancy element is moored to the ground by a vertical cable. The buoyancy element is subject to larger hydrodynamic loads, and these loads can be a design limitation for this configuration.

Steep Wave

Distributed buoyancy elements create a subsurface loop similar to the Lazy wave configuration. The difference from the Lazy wave configuration is that instead of ending horizontally on the seabed, the riser terminates vertically into a structure fixed on the seabed, see Figure 2.9. This can be useful if several risers are needed in a small area, as sliding along the seabed is prevented in such a case. The arch is

placed higher than for Lazy wave, as more buoyancy is applied to prevent stresses at the connection point at the seabed. This causes the configuration to be less desirable for fields with large current forces.

Steep S

The Steep S configuration is also terminated straight into a fixed structure at the seabed like the Steep wave, and it has one large buoyancy element like the Lazy S configuration. The difference from the Lazy S is the termination, and the mooring is not necessary in this case as the riser end is fixed to the seafloor.

2.5.3 Top-tensioned Risers

Top-tensioned risers (TTR) are completely vertical and placed directly underneath the floating facility. It is desirable to obtain constant tension in the risers. The vessel will move, and to compensate for adverse effects of vessel motion, and thus the vertical displacement between riser and connection point at floater, hydraulic heave compensation is utilized (DNV (2010c)). The vertical motion compensator ensures minimal dynamic tension variation by expanding and contracting with the facility's movements (Nielsen (2007)). A disadvantage with this riser concept is the price of such a motion compensator.

2.5.4 Hybrid Riser System

By combining the flexibility of a compliant system with heave compensation, a hybrid riser system is obtained. The most common way to combine these are through a vertical riser column with heave compensation, going from the sea-

floor to just below the surface. They are attached to a buoyancy tank at the top. Here, flexible risers are connected to the facility above, see Figure 2.10. The buoyancy tank ensures that the vertical risers keep the desired tension. This system requires careful evaluation of hydrodynamic coefficients, and the possibilities of VIV occurrence must be considered (DNV (2010c)).

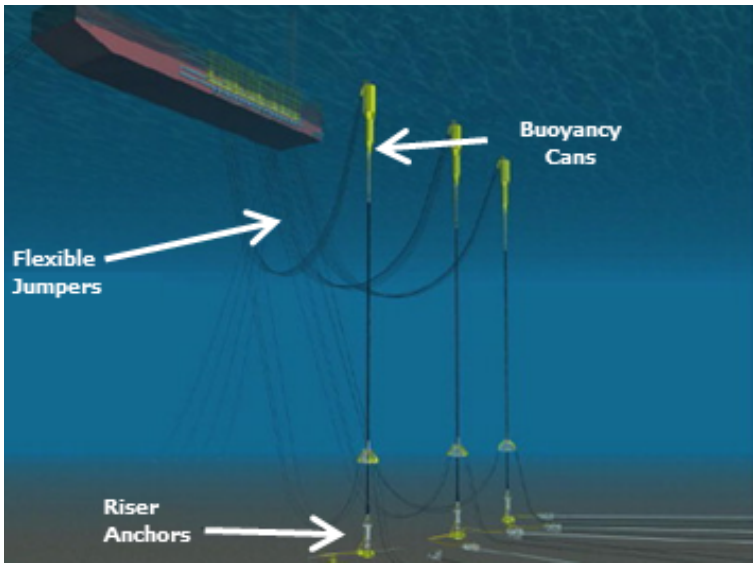

Figure 2.10: Hybrid Riser Tower (GATE (2015))

Chapter 3

The Goliat Field

The Goliat Field is located in the Barents Sea, off the Norwegian coast, about 50 kilometers south-east of Snøhvit. The field was discovered in 2000, when the first exploration well was drilled. The water depth in the area varies from 380 (Sevan Marine (2016)) to 420 (Holm (2016a)) metres.

The Goliat project is the first oil-producing field to start production in the Barents Sea (PR Newswire (2013)). It is also the nothernmost oil production site in the world (ENI (2016b)). The production license is owned by operator Eni Norge (65 %) and partner Statoil Petroleum (35 %).

The two main reservoirs constituting the Goliat Field are the Kobbe formation and the Realgrunnen group. These reservoirs both contain oil, and have an overlying gas cap. The Kobbe formation is located 1100 metres below the sea surface, and the Realgrunnen group lies at a depth of 1800 metres (ENI (2015)). In two other formations in the field, Snadd and Klappmyss, minor oil discoveries have been made. The production of the Goliat field is expected to reach nearly 100 000 barrels of oil daily. The total reservoir is estimated to contain around 180 million

barrels (ENI (2016a)).

3.1 Environmental Data

The Goliat field is located in the Barents Sea, approximately 88 kilometres north-west of Hammerfest, where Eni Norge has established an operations organisation that will operate the field (ENI (2016b)), and 219 kilometres north-east of Tromsø. Data for the Goliat field is given in Table 3.1.

Table 3.1: Data for the Goliat Field (Iden et al. (2012)), (Holm (2016a)), (Sevan Marine (2016))

Parameter	**Value**	**Unit**
Location	71.23° N, 22.21° E	
Water depth	380-420	[m]

3.2 Goliat FPSO Sevan 1000

The preferred concept for the floating production platform for the Goliat Field, is the Norwegian Sevan 1000 FPSO concept. The Goliat FPSO is based on this design, and the structure is winterized and built to withstand the environmental conditions in the Barents Sea (Sevan Marine (2016)), which can include ice hazards (ENI (2016b)). The challenges connected to ice are described in Section 3.3.3. This Goliat FPSO is the most advanced and largest cylindrical production platform in the world (ENI (2016b)). Technical data for the platform is given in Table 3.2, where LOA is Length Over All, and D is the diameter. An illustration of the platform can be seen in Figure 3.1.

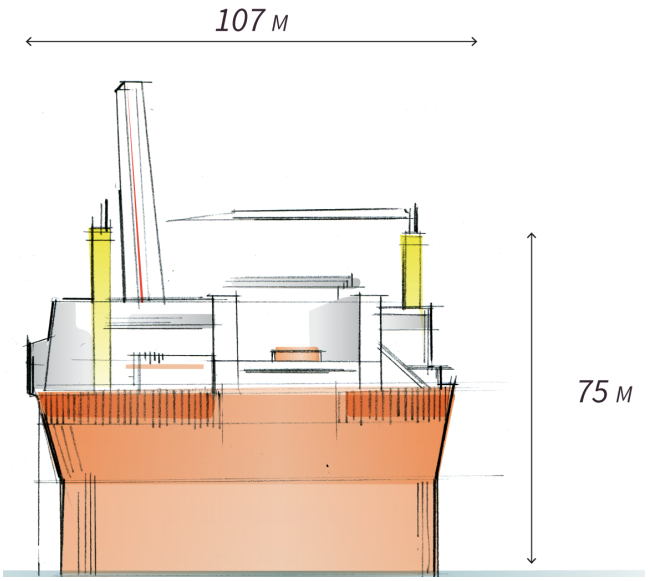

Figure 3.1: Illustration of the Goliat FPSO (Alfieri (2016))

Table 3.2: Technical data for Sevan 1000 FPSO for Goliat (Sevan Marine (2016)). The displacement corresponds to a 30.5 metre draught.

Parameter	**Value**	**Unit**
LOA (bilge box)	112	[m]
LOA (process deck)	107	[m]
D in waterline	90	[m]
Displacement	210 000	[tonnes]

The production will make use of subsea installations consisting of 22 wells. Twelve of these are production wells, seven are used to re-inject produced water into the reservoir and three wells are used for gas injection (Alfieri (2016)). To ensure station keeping, the FPSO is moored to the seabed through 14 mooring lines (Alfieri (2016)) using spread mooring (Sevan Marine (2016)), and flexible risers are used for transportation of production fluids between the wells and the platform.

3.3 Operational Challenges in the Barents Sea

Operating in arctic areas involves technical and environmental challenges. The Norwegian Meteorological Institute has provided data that shows a record of larger wave heights on the Statfjord field in the North Sea, than what has been measuren in the Barents Sea and offshore Lofoten and Vesterålen (ENI (2011)). In other words, existing technology should be sufficient to handle the rough sea in itself, but there are other challenges connected to arctic engineering. When comparing the Barents Sea and the coast off Nordland and Troms with the North Sea, the main difference is the danger of icing resulting from sea spray at low temperatures combined with wind (ENI (2011)). Other challenges are visibitily, polar low-pressure areas and remoteness. These challenges are discussed in this section, with emphasis on environmental conditions on the Goliat field.

3.3.1 Temperature

The high latitude and absence of direct sunlight in wintertime will cause low temperatures in the Barents Sea. In the south-western parts, the Gulf Stream causes higher temperatures than what is registered in other areas at similar latitudes (PSA (2014a)). For the Goliat area, the air temperature, measured 2 metres above the sea surface, will be maximum 15.6 °C and minimum -12.8 °C (Iden et al. (2012)). The sea surface temperature varies between a maximum value of 13.6 °C and a minimum value of 3.0 °C. These numbers are based on records for the period 1958-2011.

If a person should fall over board, hypothermia, which means obtaining a dangerously low body temperatur, occurs more quickly the lower the water temperature. In order to stay alive in the event of such an accident, a special survival suit has

been designed for use on Norwegian offshore facilities operating in the far north (PSA (2014a)).

3.3.2 Wind

As described before, the measured temperature in the area is higher than for other places with similar latitudes, but the wind will create a sensation of colder temperatures than what is measured. A wind chill scale is used to convert the measured temperature and wind conditions into a percieved temperature (PSA (2014a)). The US National Weather Service 2001 version of the wind chill index is given in Equation (3.1) (Palmer and Croasdale (2012)), where T_{WC} is the wind chill index, the experienced temperature, and T_a is the air temperature, both given in [°C]. V is the wind speed given in [km/hour], measured at a 10 metre reference height. This index is also used to calculate the risk of injuries related to cold weather (PSA (2014a)).

$$T_{WC} = 13.12 + 0.6215T_a - 11.37V^{0.16} + 0.3965T_aV^{0.16} \tag{3.1}$$

3.3.3 Sea Ice and Icing

Due to the Gulf Stream (PSA (2014b)), the area of the Barents Sea in which the Goliat platform is located, is ice-free under normal weather conditions (Alfieri (2016)). At this latitude, the occurence of ice still needs to be considered, as an ice collision poses a serious threat to installations. There are three different kinds of ice related hazards in arctic areas. These are icing, sea ice and icebergs.

Icing is caused by sea spray, supercooled rain or wet snow in combination with

low temperatures and strong winds. This phenomenon can result in the accumulation of ice on vessels, and icing of equipment on deck and installations (PSA (2014a)). Icing is mainly an inshore phenomenon, occuring in cold weather when strong, cold winds from the south and south-east are present near the coast. This also applies to the part of the Barents Sea where there is offshore activity. These weather conditions are most common in the late winter season, and will ususally last a few days each time (ENI (2011)). Icing can result in equpment being temporarily out of use, or even destroyed. Personal protective gear and safety devices can freeze. As a worst case scenario, vessels can obtain an unstable condition (PSA (2014a)). Figure 3.2 shows a severe case of icing on a cargo boat.

Figure 3.2: Illustration photo (*De-icing a cargo boat* (2010))

Sea ice is frozen ocean water. It has a complex structure as a result of salt influence and temperature gradient. When ice is forming, small crystals are formed in the water. These crystals connect to each other and form long strings of ice. If the sea is calm, these fragments will connect together and create a sheet. To begin with, this is a transparent sheet, but as the thickness increases, the ice will be darker and less transparent. Sea ice in calm waters is often covered with snow. If wind

or waves occur, the sea ice will be broken into fragments. These can be pushed agains each other, and some fragments might be pushed into the sea or lifted up. These phenomena are respectively referred to as keel and sail. When these ice fragments freeze together again, an ice ridge is created. Such ridges can have a keel stretching up to 40 metres down into the sea, and a sail up to 10 metres above sea level (Palmer and Croasdale (2012)). Seawater freezes around -1.8 °C (PSA (2014b)).

Icebergs are pieces of ice that have broken off a glacier, an ice shelf or a larger iceberg. These are formed on land and consist of freshwater. Because of this, the icebergs are harder than sea ice, as the salt in the sea ice ensures a softer ice type. Icebergs are most common in the North Atlantic and around Antarctica (NSIDC (2016)).

An incident with sea ice or icebergs occuring will as a worst case require a disconnection of the floating unit, and for the installations to be moved away. Another remedy against icebergs could be to tow the iceberg away from collision course. On the Goliat field, the probability of ice is considered sufficiently low, so that disconnection gear is not a requirement (PSA (2014b)).

3.3.4 Visibility

At high latitudes, visibility might be reduced due to various factors; fog, polar darkness and whiteout due to snowfall will decrease visibility.

Fog ususally occurs when the air near the ground is cooled down due to radiative cooling at the surface. Water will form droplets as a result of condensation. The temperature will be lowest closest to the ground, and increase with height. Particles in the air will assist the sepration of liquid and gas, contributing to the

creation of fog (Palmer and Croasdale (2012)). Continuous fog will prevent transportation, operation and construction in arctic regions.

In the winter season, the sun never rises north of the Arctic Circle. This phenomenon is called *Polar darkess*, and it lasts longer the further north one gets. At the North Pole, the sun remains below the horizon for six months each year, and it never sets for the other six months. Polar darkness is not absolute throughout the entire day, and sunligh might spread and scatter in the atmosphere, which in turn will illuminate the areas below. How this twilight effect will act, depends how many degrees under the horizon the sun is located. Some areas experience no twilight, and the darkness is complete for a long period of time. This is for instance the case in Longyearbyen (PSA (2014c)).

The phenomenon known as whiteout is reduced visibility due to heavy snowfall. The contrasts are low, and in severe cases, the horizon will be invisible, and visual orientation can be impossible.

Detecting and recovering oil in the darkness is possible when correct equipment is used. Infrared cameras, radar and satellite systems have been developed, tested and are successfully in use in the industry today (ENI (2011)).

3.3.5 Polar Low-pressure Areas

Polar low-pressure areas is a phenomenon occuring in the northern hemisphere. The condition occurs when cold winds blow across warmer sea water, and as this air is heated, it rises. More cold air is drawn in under the risen air, and a small indentation is created in the water. This indentation can vary in length from about 100 to 500 kilometres. Such depressions in the sea can move fast, with speeds of about 28-46 km/h. Polar lows can lead to rapid changes in the wind speed,

and wave heights can increase five metres in less than an hour, but the condition will also cease quickly, usually within 18 hours (PSA (2014d)). This weather phenomenon can be hard to detect. They are often too small to be detected by normal weather forecast, and are hence not discovered until observed in satellite photographs (ENI (2011)).

3.3.6 Remoteness

Little infrastructure and large distances can be a problem for communication, medical assistance, evacuation and rescue capacity. Before the Goliat field was established, the only development in the area was Snøhvit, which is entirely subsea. Several requirements must be met prior to operation start on Goliat, the first fixed furface installation in the area. A helicopter with a range of 340 kilometres is stationed in Hammerfest. As the Goliat platform is located only 88 kilometres from this base, a return flight would be no problem, should the helicopter be unable to land and refuel on the platform. The location furtherst north studied for petroleum activities is on the other hand more than 450 kilometres out, which would require a different solution (PSA (2014e)).

North of the 70th parallell, satellite coverage starts to weaken, and at 74°N it is lacking due to the curvature of the earth. Fixed installations can use permanent fibreoptic cabling, but for drilling rigs, this is a severe problemt. Electrical and electromagnetic storms can reduce the signal for GPS and cause magnetic disturbances for compasses. This will naturally reduce the navigation possibilities, and for instance, locating evacuated personell can be a challenge (PSA (2014e)).

Chapter 4

Software Description

In order to create a platform model, and then perform a hydrodynamic analysis on this model, relevant software packages must be utilized. In this thesis, the DNV GL's Sesam package is used to perform these procedures. Further, a riser analysis is carried out by use of the software RIFLEX, a part of Sima. Sima is a software owned, developed and maintained by Marintek.

In this chapter, a brief description of the Sesam modules is included, as well a more thorough description of RIFLEX in Section 4.3. Finally, a short description of MATLAB follows.

4.1 Sesam GeniE

Sesam GeniE is an offshore structural engineering software tool for design and analysis of fixed and floating structures. The software is based on the finite element method (FEM), and it can be used for static and dynamic analyses and for design iteration processes. Other analyses within offshore and marine structural

engineering are also available.

GeniE may be used to create panel models. A panel model defines the outer wetted surface and can be used when performing stability and hydrodynamic wave load analyses in the software HydroD, which is described in Section 4.2. Ususally, a coarser mesh density is applied for panel models than for structural analysis models. One option is that no mass model is created in GeniE. These properties will in such a case be assigned to the model in HydroD. Another option is to create the mass model in GeniE, before exporting to model for further analyses (DNV (2011)).

4.2 Sesam HydroD

Sesam HydroD is a software utilized for stability and hydrodynamic analyses and ballasting of offshore structures. It can be used for both fixed and floating structures such as gravity-based platforms, barges, ships and floating production platforms. One of the benefits of the program is the possibility of running stability analysis, frequency domain analysis and time domain analysis on the same model. The result loads can be used further in structural analyses. In the software, several non-linearities are uncluded (DNV-GL (2013)).

In Sesam HydroD, the Wadam software module uses linear frequency domain methods to calculate wave-structure interaction on panel models or beam models created by GeniE (DNV-GL (2016)).

4.3 RIFLEX

RIFLEX is a software utilized for both static and dynamic analyses of long, slender structures, for instance mooring lines, pipelines, flexible risers, conventional steel risers (Marintek (2015)) and umbilicals (Marintek (2011)). In marine applications, the slender structures often have complex cross-sections with non-linear properties (Marintek (2011)). Other slender structure characteristics are small bending stiffness and large deflections. How the software system is built up, is described in Section 4.3.1. The structural analysis part of RIFLEX is based on FEM, which is described in Section 4.3.2.

4.3.1 System Overview

The structure of the computer program is based on modules. These modules have different functions, and communicate through a file system. This way, time consumption for an analysis process is reduced. The modules are described in the following, based on information from *RIFLEX Theory Manual* (Marintek (2015)) and *RIFLEX User Manual* (Marintek (2011)). An illustration of the program structure can be seen in Figure 4.1.

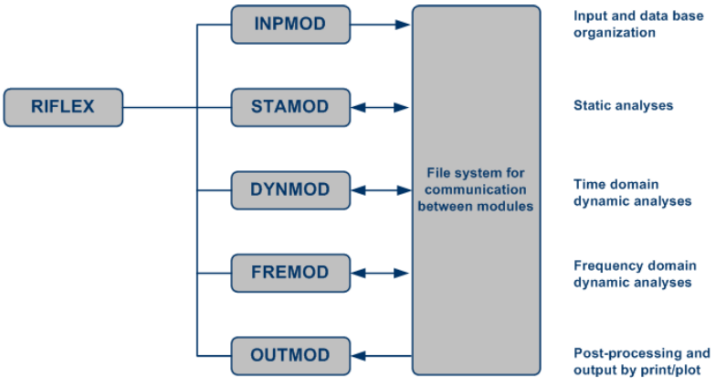

Figure 4.1: Structure of program system (Marintek (2011))

INPMOD

INPMOD is the pre-processor that reads input data. In this module, information, like material properties and environmental loads, are organized in a database to be used by the succeeding modules. When this is performed, analyses can be performed by the other modules without running the *INPMOD* module again.

STAMOD

Based on system data retrieved from *INPMOD*, the *STAMOD* module is used to perform different types of static analyses, where the results can be retrieved directly. It is also used to calculate the initial configuration for subsequent dynamic analyses, as well as generating element mesh, stress free configuration and key data needed in a finite element analysis.

DYNMOD

Dynamic analyses in the time domain are performed through the module *DYNMOD*. Such analyses are based on the final static configuration and environmental data, as well as motion applied as forced displacements. Natural frequencies and modeshapes can also be calculated by this module. Response time series are saved for post-processing by the two modules *OUTMOD* and *PLOMOD*. Most results from the dynamic analyses can be retrieved and presented as tables and graphs. Some exceptions require further analyses. In this module, several dynamic analyses can be performed without having to rerun the *STAMOD* and *INPMOD* modules.

OUTMOD

Results from static and dynamic analyses are stored as result files. These files can be retrieved, analysed further and presented by means of the module *OUTMOD*. Plots can be stored on files, and these can be retrieved by *PLOMOD*. Time series can also be exported through standardised file formats to be postprocessed by statistical analysis software.

PLOMOD

PLOMOD is a post-processing plotting module. Here, plots generated by *OUTMOD* can be transformed into graphic output. Visualization of the dynamic behaviour of the system is available through an animation tool.

4.3.2 The Finite Element Method

FEM is a numerical method to solve structural engineering problems. A model is discretised intro a finite number of elements. Each element is subject to analysis, and the solutions are assembled into a total solution for the entire structure.

Essential features for satisfactory modelling and analysis of marine structures, listed below, are included in the finite element method formulation in RIFLEX (Marintek (2015)).

- Unlimited number of rigid body motions in 3D space
- Small strain theory for both beam element and bar elements
- Both beam and bar elements are utilized in system modelling
- Description of non-linear material properties

- Contribution of axial force to transverse stiffness, which means there is a stiffness contribution from both material properties and geometric stiffness

- Description of arbitrary system topology allowed through general element assembly. This also enables varying cross-sectional properties, arbitraty boundary conditions at supports, prescribed support displacement and specified external forces.

The listed features are fundemental for modelling of slender structures in general, and is hence applied for both static and dynamic analyses.

Figure 4.2 illustrates how a line is discretised in RIFLEX. The supernodes are branching points with specified boundary conditions, and the line is a structure suspended between two supernodes. A segment is a uniform part of the line with identical properties. Each segment is divided into a finite number of elements (Marintek (2011)).

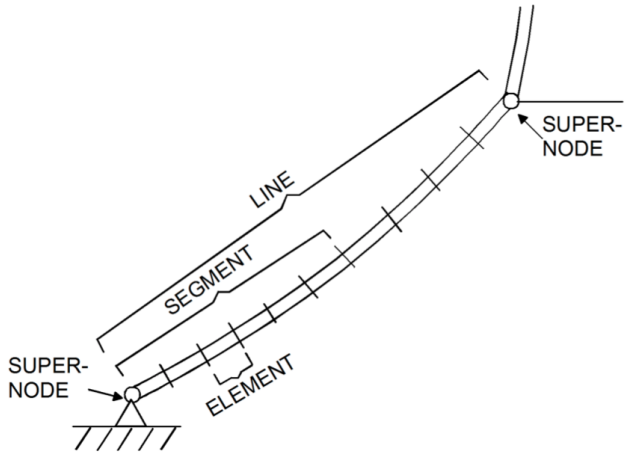

Figure 4.2: System definition terms (Marintek (2011))

4.3.3 Static Analyses

The static analysis is based on a complete non-linear finite element analysis. To reduce computation time, a pre-processor based on catenary theory is implemented, as this gives a good starting point for the non-linear analysis (Marintek (2011)). This feature also enables analysing simple problems without using the finite element method.

Static Catenary Analysis

Using the finite element method to perform an analysis can be time-consuming. A less time-consuming method is utilizing a 2D static catenary analysis as a supplement. Standard systems SA, SB, SC, SD, CA and CB can be utilized for this purpose. A description of these follows in Table 4.1. SA, SB, SC and SD are single configurations, while CA and CB are coupled systems. The solutions of CA and CB should only be used as a starting point for finite element solutions, as equlibrium is not obtained (Marintek (2015)).

Table 4.1: Riser configurations in RIFLEX

SA	One point seabed contact, steep configurations
SB	Tangential seabed contact, lazy configurations
SC	Free lower end
SD	Free upper end
CA	Coupled system, parallell risers
CB	Coupled system, branched riser from support column

Catenary analyses give exact solutions for single line cables, but does not consider bending stiffness. For systems that are influenced by bending stiffness to a large

extent, a catenary analysis will only serve as an approximation.

A catenary element analysis' main purpose is to calculate the static equilibrium configuiration of a single line, when boundary conditions are defined at both ends, and the loading is uniform (Marintek (2011)). If the boundary conditions are unknown at one end, an iterative correction of the unknown boundary conditions can be performed in order to satisfy known boundary conditions at the other end. This is known as the shooting method (Marintek (2015)). If no current loading is present, the initial value problem can be solved, one segment at the time, by catenary equilibrium calculations. This ensures an exact catenary solution. If current is the dominating loading mechanism, the catenary analysis may be unstable, but for most cases with a present current loading, an approximate solution can be found (Marintek (2015)), and further non-linear static analyses can be performed.

Static Finite Element Analysis

The nodal displacements of a discretised finite element model determines its condition. The purpose of a finite element static analysis is to ensure nodal displacements such that static equilibrium is obtained for the system. The general system of equations to solve is given in Equation (4.1), where $\boldsymbol{R}^S(\boldsymbol{r})$ is the internal reaction force vector and $\boldsymbol{R}^E(\boldsymbol{r})$ are the external force vector. They are generally non-linear functions, dependent on the nodal displacement vector $\boldsymbol{r}$ that describes all degrees of freedom in a system. When Equation (4.1) is solved, the solution gives the static equilibrium configuration (Marintek (2015)).

$$\boldsymbol{R}^S(\boldsymbol{r}) = \boldsymbol{R}^E(\boldsymbol{r}) \tag{4.1}$$

The static equilibrium is found numerically by application of an incremental loading procedure. Here, equilibrium iteration is performed for each load step, using the static configuration from previous load step as the starting point. This method is used when the finite element analysis starts from a stressfree configuration (Marintek (2015)).

Another approach is to apply the catenary solution as a start configuration for the finite element analysis, as discribed previous in this section. This method provides a reduction in computation time.

4.3.4 Dynamic Analysis

Similarly as for a static finite element analysis, the dynamic analysis is based on an equlibrium equation, dependent on the discretized model's nodal behaviour. This equilibrium equation is given in Equation (4.2), where $\boldsymbol{R}^I$ is the inertia force vector, $\boldsymbol{R}^D$ is the damping force vector, $\boldsymbol{R}^S$ is the structural reaction force vector and $\boldsymbol{R}^E$ is the external force vector. These are functions of the struture's nodal displacement $\boldsymbol{r}$, velocity $\dot{\boldsymbol{r}}$ and acceleration $\ddot{\boldsymbol{r}}$ as well as time $\boldsymbol{t}$. The force vectors are again dependent on different physical contributions. Equation (4.2) is a non-linear system of differential equations.

$$\boldsymbol{R}^I(\boldsymbol{r},\ddot{\boldsymbol{r}},\boldsymbol{t}) + \boldsymbol{R}^D(\boldsymbol{r},\dot{\boldsymbol{r}},\boldsymbol{t}) + \boldsymbol{R}^S(\boldsymbol{r},\boldsymbol{t}) = \boldsymbol{R}^E(\boldsymbol{r},\dot{\boldsymbol{r}},\boldsymbol{t}) \tag{4.2}$$

If a dynamic analysis is performed on a structure, a judgement must be made on whether a non-linear analysis is required, or if a linearized dynamic analysis is sufficient. For instance, analyses involving certain flexible risers, umbilicals and pipelines under installation would suggest a non-linear analysis being performen, while standard flexible riser configurations and anchor lines in normal operating

conditions only would require a linearized analysis (Marintek (2015)).

Linearized Dynamic Analysis

Linearized dynamic analyses are sufficiently accurate for a wide range of systems. This type of analysis is particularly attractive in cases with moderate structural non-linearity, as non-linear hydrodynamic looading is included in this analysis type. This means that it is a good approach where the external hydrodynamic loading is the main source to non-linearities. Such cases include standard flexible riser configurations and anchor lines in normal operating conditions. This type of analysis requires 10% of the computation time compared to non-linear dynamic analysis. For critical cases, non-linear verification of results obtained should be considered (Marintek (2015)).

Non-linear Dynamic Analysis

Some non-linear phenomena result in a non-linear analysis being required. For instance, a non-linear analysis is required for release and rupture analysis. Both anchor lines and flexible riser systems are subject to such an analysis (Marintek (2015)). For other situations, a non-linear analysis would be desired as a verification of a linearized analysis. Non-linear analyses are time-consuming, and is hence desired to apply only when neccessary. Some of the most important non-linear effects regarding marine slender structures are geometric stiffness, non-linear material properties, contact problems and hydrodynamic loading according to Morison's equation expressed by relative velocities. The Morison's equation is further described in Section 5.2.

Time Domain and Frequency Domain Analyses

A time domain analysis gives a representation of how the response of a structure varies with respect to time. Such an analysis performs a step by step numerical integration of the dynamic equilibrium equation. The time domain analysis can be either completely non-linear, or a non-linear approach can be applied.

A frequency domain analysis investigates a structure's response for different wave frequencies. It is based on the linearized dynamic equilibrium equation. In this case, the hydrodynamic loading is also linearized (Marintek (2015)).

4.4 MATLAB

MATLAB is short for matrix laboratory. It is a programming tool often used in mathematical contexts. It uses its own programming language, but can communicate with programs written in other languages. In this thesis, MATLAB is used to process results by creating graphic plots.

Chapter 5

Loading Mechanism

During operation, a floating structure and its accociated components are subject to various environmental loads. These loads act on the body and riser column, and they influence the forces and bending moments within the structures. It is important to identify these loading mechanisms, in order for a design to withstand the forces it is exposed to.

5.1 Environmental Loads

Offshore structures are subject to various external forces acting on the floating structure and its risers and mooring lines, causing motion in the six degrees of freedom. Environmental loads vary throughout the period considered in an analysis. This includes variation in both magnitude and direction. The hydrodynamic loads, waves and current, falls into this category, along with inertia forces, wind and tidal effects. In addition, extreme weather and phenomena, like snow and ice and earthquakes, are considered environmental loads. Wind, waves and current

are excitation forces that directly affect the response of the structure.

5.1.1 Wind

Wind can cause slowly-varying oscillations of floating structures with high natural periods. This happens as a result of wind gusts with considerable energy at similar, high periods. Wind is commonly considered constant in a design situation, at least in the early stages of the process. In cases where risers, or other completely submerged structures, are considered, wind will not affect the structure directly, but wind forces exterted on the vessel can impact the riser or mooring line response and motion.

5.1.2 Waves

Waves are a combination of two contributions, wind waves and swell. Wind waves are a result of the local wind transferring its energy to the water, while swell is not affected by the local wind at the time. It is a result of wind-generated waves created at another time and place. Swell waves usually have very large wavelengths. Wave forces are significant in analyses of marine structures, as they result in considerable motions and forces on the structures. In structural analyses, waves vary with time. It is common to include wind waves alone or in combination with swell waves.

Regular Wave Theory

Regular wave theory is a linear theory based on potential theory. Potential theory means that water is assumed to be irrotational, inviscid and incompressible. Vis-

cous effects are hence neglected in potential theory. In linear theory, horizontal seabed and sea surface of infinite size is assumed.

$$\xi = \xi_a \sin(\omega t - kx) \tag{5.1}$$

A regular wave has only one wave frequency and one wave height. The wave profile of a regular wave propagating in x-direction can be described from Equation (5.1), where ξ is the wave profile and ξ_a is the wave amplitude. ω is the circular frequency, t is time and k is the wave number.

The JONSWAP Spectrum

An irregular sea state is a superposition of a large number of regular waves. This irregular sea can be described by using a sea spectrum, and it gives a more realistic representation of the sea state than a regular wave. A commonly used sea spectrum is the JONSWAP spectrum. This is frequently applied for wind seas, and describe wind sea condition that often occur for harsh sea states (DNV (2010b)).

5.1.3 Current

Current can be described as a large block of water moving, mainly horizontally, in the ocean. It is influenced by wind, tides, surges, location and Stokes drift (Faltinsen (1990)). Time dependent current variation can be described in a dynamic analysis. Still, the current velocity is usually assumed to be constant with time in an analysis situation, as this generally will give a satisfactory level of detail in the result. Variation along the z-axis is described by a current profile where the current velocity can vary with depth, and at a certain depth set to be zero. The direction can also vary, and is assumed to be zero in vertical direction at all times.

For a riser analysis, the current is a crusial environmental parameter as it affects the riser system at larger depths than wind waves.

5.1.4 Damping

Exciting forces are energy transported from the water to the structure, and damping can, in potential theory, be described as energy leaving a system as waves radiating away from the body, i.e. energy is transported from the structure to the water. Damping contributes to limit the response oscillation of a structure, after being exposed to external loads. If no damping is present in a system, and resonance occurs, the response amplitude will increase indefinetely. Resonance is recognized by extreme oscillation amplitude, and occurs if the frequency of the excitation force is close to the natural frequency of the structure. In reality, all structures have a certain damping level, but close to resonance, large responses and structural damages can occur. Because of this, it is important to design structures such that resonance is avoided (Larsen (2015)). Hence, when calculating dynamic response, damping is an important factor. In general, it is hard to calculate the exact damping for a floating production system. For stiffness dominated or inertia dominated systems, this is not crucial, but close to resonance, the damping level is essencial for the response (Larsen (2015)). A system is stiffness dominated when the frequency of the excitation force is lower than the natural frequency of the system. The magnitude of the response is then determined by the stiffness in the system. However, if the frequency of the excitation force is greater than the natural frequency of the system, the response of the system will be inertia dominated. Floating production units are typically inertia dominated with large eigenperiods (DNV (2010c)).

The damping consists of several contributions. These are hydrodynamic damp-

ing, soil damping and structural damping. Other small damping components also exist, as contributions from air, internal fluids and friction from attachment devices. Only the hydrodynamic damping will be further discussed here, as this usually is the governing damping mechanism. The hydrodynamic damping can be divided into three categories. These are potential damping, viscous damping and damping from skin friction (Larsen (2015)).

Potential damping is, as described in this section's introduction, connected to a structures ability create waves when it oscillates. Potential forces, as well as drag forces, are resultants of a structure being exposed to pressure forces.

When the structure moves in the water, vortex shedding will occur, and this will cause viscous damping. The viscous damping is related to the drag term in Morison's equation, which is explained in Section 5.2. At locations where the water particles have large motion, the drag forces will be exciting forces. Contrary, on larger depths, where the wave effects have been reduced due to exponential decay, the drag forces will function as damping. Drag forces are further described in Section 5.2.1

Damping from skin friction is a result of shear forces between the water and a body's wet surface. This damping contribution is small, and is only significant in situations where drag forces and potential forces are small.

5.2 The Morison Equation

When calculating forces on slender structures, like for instance risers, Morison's equation can be applied. The Morison equation is a semi-empirical expression describing the force on a body in oscillating flow. The theotical basis for the equation is a mathematical derivation, but some of its components are empirically de-

termined. In this section, a cylinder is used to describe the features of this equation and its utilization, as well as when describing the drag term in Section 5.2.1. This is both due to simplicity and the fact that cylinders are highly common in a marine engineering context.

$$\mathrm{d}F = \mathrm{d}F_{inertia} + \mathrm{d}F_{drag} = \rho\pi\frac{D^2}{4}\,\mathrm{d}z C_M a_1 + \frac{\rho}{2}C_D D\,\mathrm{d}z|u|u \tag{5.2}$$

In Equation (5.2), the inline horizontal force on a strip of a cylinder is expressed. This is Morison's equation for a rigid cylinder with no movement. The equation consists of two parts. The first term is the mass term based on inertia and acceleration, and the second term is based on velocity and drag. D is the diameter of the cylinder, ρ is the water density, u and a_1 are undisturbed horizontal fluid velocity and acceleration caused by waves and current, respectively, and C_M and C_D are coefficients. C_M is the mass coefficient. For a cylinder in potential theory, $C_M = 2$, when the wavelength is large compared to the diameter of the cylidrical structure. The coefficients C_M and C_D are the parameters needing to be empirically determined, and they dependent on variables like for instance Reynolds number, surface roughness and a relative current number. These are assumed to be constant with depth (Faltinsen (1990)). The drag coefficient and drag forces are explained further in Section 5.2.1. Morison's equation is only used to calculate inline, and not transverse, forces. This means that lift forces are not considered.

$$\mathrm{d}F = \frac{1}{2}\rho C_D D\,\mathrm{d}z(u-\dot{\eta})|u-\dot{\eta}| + \rho C_M\frac{\pi D^2}{4}\,\mathrm{d}z\,a_1 - \rho(C_M-1)\frac{\pi D^2}{4}\,\mathrm{d}z\,\ddot{\eta}_1 \tag{5.3}$$

When considering the relative velocity between a moving cylinder and the fluid, Morison's equation can be expressed as seen in Equation (5.3), where $\dot{\eta}$ and $\ddot{\eta}$ is

the velocity and acceleration of the cylinder, respectively (Faltinsen (1990)).

5.2.1 Drag Forces

It is important to include a good representation of the drag forces from waves in the analysis or design phase of marine structures. Usually, Morison's equation is used to calculate this force (NTNU (2015)). Figure 5.1 displays a vertical pile. This figure can serve as an illustration of how forces will act on a riser. If the structure's motions is sufficiently small compared to the incoming wave amplitude, the drag force can be calculated directly without considering the body's motion.

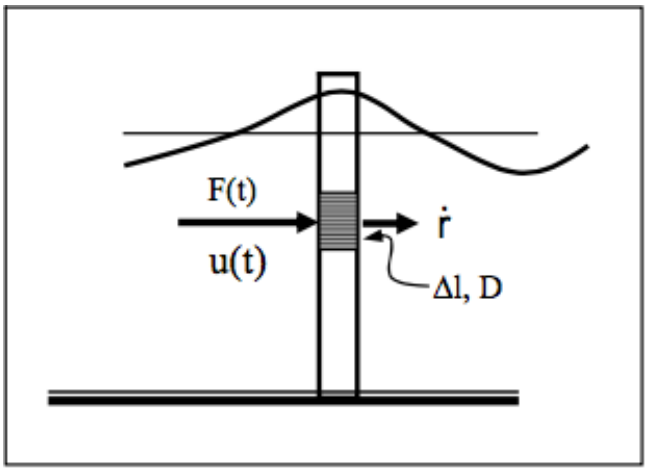

Figure 5.1: Forces on a vertical pile (NTNU (2015))

There are two types of drag coefficients, linear and quadratic. For dynamic analyses in the time domain, a quadratic drag coefficient is utilized. For analyses in the frequency domain, the drag coefficient needs to be linearized. This is due to the assumption that the response amplitude is proportional to the wave amplitude at each frequency. In a time domain analysis, the drag forces will be calculated from Morison's equation at each time step, and these are hence automatically correct. For the frequency domain, there are simplified ways of calculating

drag force, as long as the motions of the structure are small. The load and response is calculated for each component, and added together. If, however, the structure's velocity becomes of significant magnitude compared to the wave induced velocity, superposition is not valid. Such a case would require full linearization of the drag forces (NTNU (2015)).

The drag coefficient is dependend on three parameters, which are the Keulegan-Carpenter number, Reynolds number and the roughness. The definition for the Keulegan-Carpenter number, K_C, is found in Equation (5.4), where T is the wave period, D is the diameter and v_m is the the maximum wave orbital particle velocity. If the structure is moving, v_m is the relative velocity between the wave and the member. K_C is varies with ocean depth. R_e is the Reynolds number, and is defined as seen in Equation (5.5). u is the total flow velocity and ν is the fluid kinematic viscosity. The roughness, Δ, is a ratio between the structure diameter and the roughness height of the surface k, as seen in Equation (5.6).

$$K_C = v_m \frac{T}{D} \tag{5.4}$$

$$R_e = \frac{uD}{\nu} \tag{5.5}$$

$$\Delta = \frac{k}{D} \tag{5.6}$$

Physically, this means that the drag coefficient will vary with many parameters, and the structure's diameter will influence all of the three parameters discussed in this section. In addition, the roughness is dependent on choice of material and its processing, and it will change due to marine growth. The Reynolds number

will vary with temperature due to viscocity, and this number influences the drag, alongside the Keulegan-Carpenter number and the wave and flow velocity. In Figure 5.2, the drag coefficient's dependencies on roughness and Reynolds number are given. This graph indicates that the drag force is strongly dependent on the flow conditions and the Reynolds number.

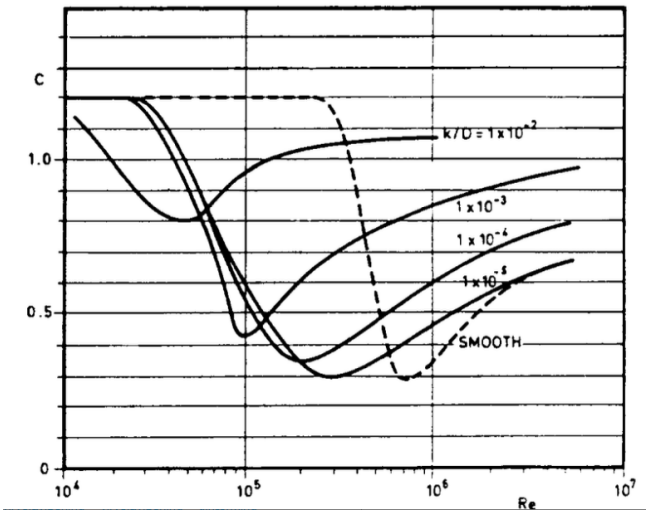

Figure 5.2: Drag coefficient for circular cylinder in steady flow (DNV (2010b))

Drag forces on slender strcutres can be both exciting and damping forces, as mentiones in Section 5.1.4. For instance, the upper part of a vertical riser can be influenced by wave induced drag forces, which are exciting forces. The lower part can experience motion induced drag that will dampen the motion (Larsen (2015)). In such cases, large damping will reduce the effect of a resonance incident. The riser's cross-sectional properties strongly affects the physical behaviour of the structure's damping properties (Marintek (2015)).

5.2.2 Mass Forces

The mass coefficient C_M is defined in Equation (5.7) (DNV (2010b)), where C_A is the non-dimensional added mass. The mass coefficient is hence also non-dimensional. The added mass coefficient is dependent on the frequency of oscillation, and the free surface may have an effect if the structure is close to the surface (DNV (2010b)).

$$C_M = 1 + C_A \tag{5.7}$$

In the same way as for the drag coefficient described in Section 5.2.1, K_C and roughness influences the added mass.When calculating the force from Morison's equation, the mass term is in general dependent on the choice of mass coefficient, as well as structure geometry and flow velocity. If structuce motion is present, its velocity and acceleration will also affect the mass force.

5.3 Effective Tension

When risers are subject to analysis, effective tension in the riser is an important measure. It is necessary to account for the fact that the riser is submerged in a fluid, and that it contains internal fluid as well. Hence, the tension occurs not only due to the weight, but also due to outer pressure. The result is a combination of compression and axial forces, i.e. transversal contraction. The internal pressure counteracts this effect. This is expressed in Equation (5.8), where T_w is the wall tension. The pressure on the inside and outside is denoted p_i and p_o, respectively, while A_i and A_o are the internal and external cross-sectional areas.

$$T_e = T_w - p_i A_i + p_o A_o \tag{5.8}$$

Chapter 6

Rules and Regulations

In this thesis, rules and recommendations from DNV are referred to. In this chapter, some relevant standards are listed and shortly presented.

DNV-OS-F201- Dynamic risers

This offshore standard provides criteria, requirements and guidance on design and analysis of riser systems subject to static and dynamic loading (DNV (2010e)). It describes design principles, design criteria, loading mechanisms and analysis methodology for extreme combined load effect assessment and fatigue analysis. It is applicable to all categories of risers.

DNV-RP-F202 - Composite risers

This recomended practice contains information on the design philosophy, loads and global analysis aspects valid for risers made of composite materials (DNV (2010a)). A composite material consists of two, or more, different materials with

dissimilar characteristics. This is often the case for flexible risers, as they consist of steel and plastic.

DNV-RP-C205 - Environmental conditions and environmental loads

This recomended practice gives guidance considering environmental conditions in a design or analysis situation, and the impact of these loads on structures. It contains a thorough description on wave and current induced loads on slender members, such as drag and mass forces, which is highly relevant for risers.

DNV-RP-F205 - Global Performance Analysis of Deepwater Floating Structures

The term *Deepwater Floating Structures* is defined as an integrated dynamic system of a floater, risers and mooring that responds to wind, wave and current loadings in a complex way (DNV (2010c)). This is relevant to utilize when a floating production system is going to be chosen or subject to analysis.

Chapter 7

Case Study

In this part of the thesis, the parameter study is carried out. In order to perform these analyses, a structure simulating the Goliat FPSO and a flexible riser was modelled. The environment was defined, and the parameter variations were applied. The system modelling is described in Section 7.1, the environment parameters for the analyses are defined in Section 7.2 and the parameter variation is presented in Section 7.3. The results from the static and dynamic analyses are presented in Chapter 8. A discussion of these follows in Chaper 9. Finally, in Section 7.4, an analysis regarding horizontal offset is presented.

7.1 Modelling and System Description

The first modelling step was to create a platform model and identifying its characteristic motion. Next step was to adjust the riser model in the RIFLEX task, *Simple Flexible Riser*, existing in Sima, and connect the riser to the characteristic motion. The procedure is described in this section. Boundary conditions are defined in

Section 7.1.4.

7.1.1 Modelling of the Goliat FPSO

In order to find the platform's transfer functions, a model was created. In this study, the platform is simplified to be a perfect, uniform cylinder under the waterline, which means that the bilge box is ignored. Based on this simplification, and as the diameter in the water line is 90 metres, the calculated draught will be 32.2 metres. This is calculated based on the displacement of 210000 tonnes, which equals a displaced volume of $2.05 \cdot 10^5$ m^3.

First, a panel model was created utilizing Sesam GeniE. Dimensions were assigned to this model, but no mass or material properties. Figure 7.1 displays a basic schematic illustartion of the Goliat FPSO. For the panel model, only the submerged part of the hull is modelled, which is the blue part B in the figure. The dimensions corresponding to Figure 7.1 are listed in Table 7.1. The panel model created in GeniE can be seen in Figure 7.2.

Table 7.1: Dimensions on schematic illustration of the Goliat FPSO seen in Figure 7.1

	Value [m]
a	107
b	58
T	32.2
d	90

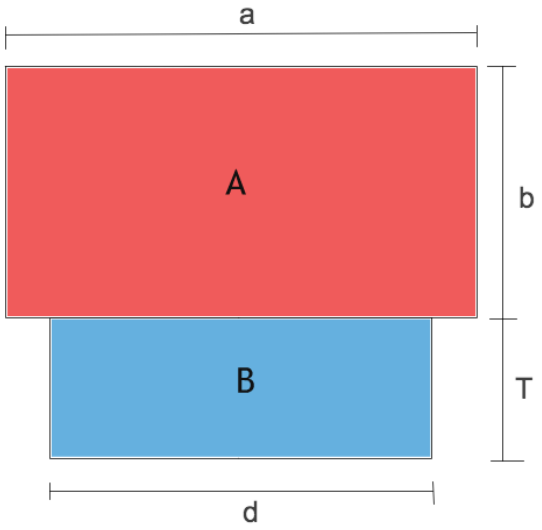

Figure 7.1: Schematic illustration of the Goliat FPSO, where B is the modelled, submerged circular hull, and A only represents the topside considering weight distribution

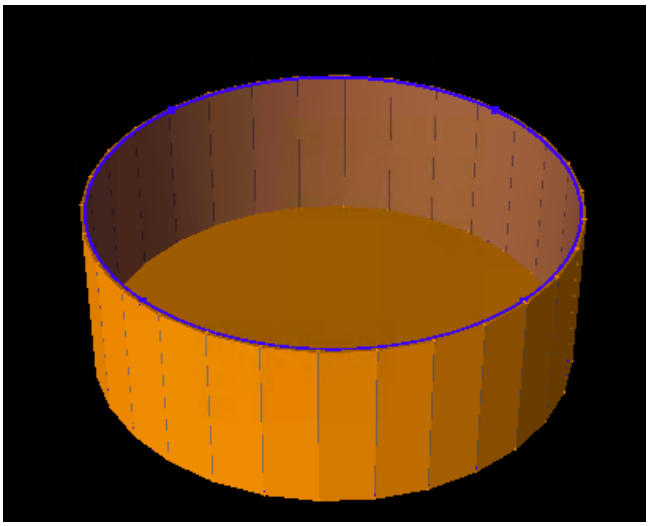

Figure 7.2: Panel model of the Goliat FPSO in GeniE

Using Sesam HydroD, a hydrodynamic analysis was perfomed. The first step was to import the panel model created in GeniE, followed by defining environmental

parameters in order to simulate a specific location. These are listed in Table 7.2. By utilizing a panel model, potential theory is applied, and viscous effects are neglected. The hydrodynamic analysis performed on the model was executed in the frequency domain.

Table 7.2: Location parameters

Parameter	**Value**	**Unit**
Gravity	9.80665	[m/s^2]
Air density	1.227	[kg/m^3]
Kinematic viscosity of air	$1.462 \cdot 10^{-5}$	[m^2/s]
Water density	1025	[kg/m^3]
Kinematic viscosity of water	$1.19 \cdot 10^{-6}$	[m^2/s]

In order to perform this analysis, it was necessary to define a mass model. When creating the model, only the part under the water is modelled. The shape of the structure above the water line not considered, except the influences of the weight distribution, and hence the location of COG. Here, this is simplified as seen in the schematic illustration of the model in Figure 7.1. COG was calculated from Equation (7.1). In this case, it is assumed that heavy ballast is used, and that 70% of the total mass is located in the lower part of platform, the blue part B in the illustration. Applying Equation (7.1), the location of COG found to be $z = -2.57$ [m].

$$\text{COG} = \frac{\sum m_i x_i}{\sum m_i} \tag{7.1}$$

$$
\begin{aligned}
I_{xx} &= \sum m_i (y_i^2 + z_i^2) \\
I_{yy} &= \sum m_i (x_i^2 + z_i^2) \\
I_{zz} &= \sum m_i (x_i^2 + y_i^2)
\end{aligned}
\tag{7.2}
$$

$$
\begin{aligned}
I_{xy} &= -\sum m_i x_i y_i \\
I_{xz} &= -\sum m_i x_i z_i \\
I_{yz} &= -\sum m_i y_i z_i
\end{aligned}
\tag{7.3}
$$

$$
R_{ij} = \sqrt{\frac{I_{ij}}{M_{tot}}} \tag{7.4}
$$

Moment of inertia is calculated from Equation (7.2), and product of inertia, which is the measure of symmetry, is calculated from Equation (7.3). Most of these are zero due to symmetry. Symmetry about the xz-plane and the yz-plane results in values found in Tables 7.3 and 7.4. The formula for radius of gyration is given in Equation (7.4).

Table 7.3: Moments and products of inertia

I_{xx}	I_{yy}	I_{zz}	I_{xy}	I_{xz}	I_{yz}
$9.11 \cdot 10^{10}$	$9.11 \cdot 10^{10}$	0.0	0.0	0.0	0.0

Table 7.4: Radius of gyration

R_{xx}	R_{yy}	R_{zz}	R_{xy}	R_{xz}	R_{yz}
20.83	20.83	0.0	0.0	0.0	0.0

The final step of the hydrodynamic analysis on the platform was to define a sea state. The 100-year return period wave for the Goliat field is H_S=16.5 [m] and T_P=18.0 [s] as stated in Table 7.5, and $T_P/\sqrt{H_S} = 4.43$, which meats the criteria for

use of the JONSWAP spectrum given by Equation (7.5) (DNV (2010b)). Within this interval, the spectrum parameter γ is given by Equation (7.6) (DNV (2010b)). The parameters for the JONSWAP spectrum can be found in Table 7.6.

Table 7.5: H_S and T_P for with a 100-year return period for position 71.23 N, 22.21 E (Goliat) (Iden et al. (2012))

Parameter	**Value**	**Unit**
H_S	16.5	[m]
T_P	18.0	[s]

$$3.6 < T_P/\sqrt{H_S} < 5 \tag{7.5}$$

$$\gamma = \exp(5.75 - 1.15\frac{T_P}{\sqrt{H_S}}) \tag{7.6}$$

Table 7.6: JONSWAP spectrum parameters (DNV (2010b))

Parameter	**Value**	**Unit**
H_S	16.5	[m]
T_P	18.0	[s]
γ	1.923	[-]
σ_a	0.07	[-]
σ_b	0.09	[-]

Due to the circular shape of the platform, responsers are independent of the wave heading, and waves were only applied from one direction. This resulted in no roll response due to choice of direction, but symmetry was defined such that the roll and pitch responses are identical.

7.1.2 Simple Flexible Riser

As a basis for the riser model subject to investigation, the *Simple Flexible Riser* was utilized. To ensure that the riser could be attached to the circular FPSO on the Goliat field, some adjustments were made to the initial riser model.

The water depth at the Goliat field is 380-420 metres (Holm (2016a)),(Sevan Marine (2016)). The analysis is performed for a 400 metre water depth. The *Simple Flexible Riser* was initially used for a water depth of 100 metres, and the model was adapted to fit the 400 metre loacation. The total riser length is 644 metres.

To model the connection between the Goliat platform simulation and the flexible riser, the platform model's transfer function, given by an RAO-file, is applied in RIFLEX. This ensures that the platform's motion pattern is imitated at the riser top, and the riser response and forces act accordingly. The platform's horisontal offset, relative to the touchdown point (TDP), was initially 300 metres, and this value is used in the parameter study. Subsequently to the parameter study, an analysis for variation of the offset was performed. This is described in Section 7.4.

The riser is modelled in three segments, ref. Figure 4.2 on page 44. The first segment is a regular flexible riser segment called *Bare Riser*, the second segment is a buoyancy section and the third is again regular riser. The riser is of the type steep wave configuration, as it is fixed to the seabed in a single point, and it has distributed buoyancy elements, ref. Figure 2.9 on page 24. This riser has the SA configuration type in RIFLEX.

Normal mass coefficient, C_M, alongside tangential mass and drag coefficient C_D^T and C_M^T are chosen as seen in Table 7.7. These are set to be constant, and the values are based on data from DNV-RP-C205. The normal drag coefficient C_D is

subject to variation, see 7.3.3.

Table 7.7: Hydrodynamic coefficients for riser

	C_M	C_D	C_D^T	C_M^T
Bare riser	1.6	Variable	0.1	0.1
Buoyancy Section	1.8	Variable	0.7	0.7

Remaining material and riser properties adopted from the RIFLEX example file. These can be found in Appendix A

7.1.3 Flexible Riser Cross-section

As decribed in Section 2.5.1 on page 23, flexible risers are complex structure with a cross-section consisting of many layers with different functions. Commonly, armour wires combined with layers of polymers, textiles and tape are utilized in order to withstand structural loads and external and internal pressure (Witz (1996)). An illustration of these layers is given in Figure 7.3.

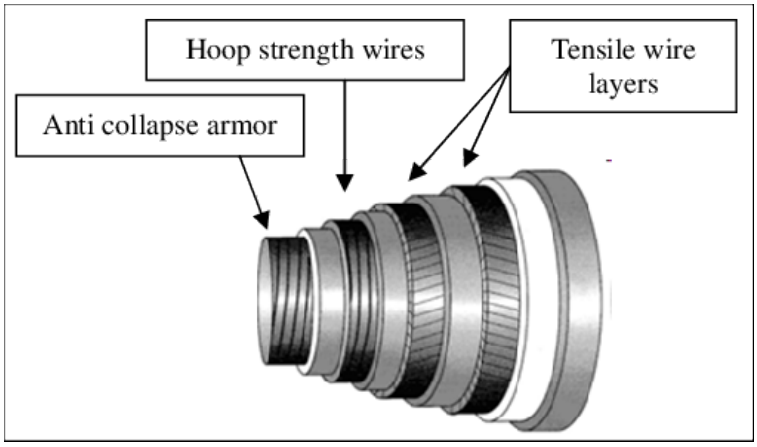

Figure 7.3: Illustration of riser cross-section (Gundersen (2012))

In this thesis, an external and internal diameter is given, along with the total dry weight of the riser given in [kg/m]. Global material properties are given, and the layers are not considered. The diameter of the riser is subject to variation, see Section 7.3.2, but the buoyancy section's diameter is constant, and has a value of 0.62 metres.

7.1.4 Boundary Conditions

The termination of the riser is steep, and this node is hence fixed to the seabed with restraints in all six degrees of freedom. The upper node represents the attachment to the vessel. For the static analysis, the riser top is restrained from moving, with the exception of rotations about the x-axis and y-axis. For the dynamic analysis, the riser hangoff node's boundary conditions are changed to enable the riser to move. All boundary conditions are listed in Table 7.8.

Table 7.8: Boundary conditions for riser

	Translations			**Rotations**		
	x	y	z	x	y	z
RiserAnchor	Fixed	Fixed	Fixed	Fixed	Fixed	Fixed
RiserHangoff, static	Fixed	Fixed	Fixed	Free	Free	Fixed
RiserHangoff, dynamic	Free	Free	Fixed	Free	Free	Free

7.2 Environment

In the RIFLEX task, the environment needs to be defined. The conditions and loads on the location are given in this section. Remaining location parameters are adopted from the RIFLEX example file. These are given in Appendix B.

7.2.1 Wind

In this analysis, wind is not included. It is assumed that the greatest effect of the wind is the creation of waves, and that the waves represent the wind. This is assumed to be satisfying as the riser is under the water line.

7.2.2 Wave

The wave condition is constant throughout the case study. A regular wave is utilized, with a return period of 100 years. Significant wave heigh H_S = 16.5 [m] is used as the wave height. The amplitude given as input to RIFLEX is then 8.3 metres, while the period is 18 seconds. The waves are propagating in the positive x-direction.

7.2.3 Current

The current is, as mentioned in Section 5.1.3 on page 53, an important parameter with respect to riser analyses. It is hence an intersting parameter to investigate in a sensitivity study. The varying current for this purpose is described further in Section 7.3.1. The value used as a reference is based on data from The Norwegian Meteorological Institute (Iden et al. (2012)).

7.2.4 Seabed Conditions

Due to insufficient data on the actual seabed conditions on the Goliat field, it is chosen to use caracteristic values taken from SINTEF (SINTEF (n.d.)), as these are correct order of magnitude. The chosen values are given in Table 7.9.

Table 7.9: Seabed conditions

Parameter	**Value**	**Unit**
Vertical stiffness	200	[kN/m^2]
Horizontal stiffness, axial	100	[kN/m^2]
Horizontal stiffness, lateral	80	[kN/m^2]
Horizontal friction, axial	0.6	[-]
Horizontal friction, lateral	0.8	[-]

7.3 Parameter Study

In this part of the study, various parameters are subject to change, in order to investigate the effects on the riser performance. The parameters to be investigated are listed below, and these are discussed further in this chapter.

- Drag coefficient
- Diameter
- Current profile

Subsequently, an additional analysis for varying position of the platform, and hence the riser top, relvative to TDP, is completed. This is described in Section 7.4.

7.3.1 Varying Current

An analysis of the riser is performed for three different current profiles. The first case is no current, the second case has a current that decreases linearly with depth, while a uniform current profile is applied as the third case. The current profiles

are listed in Table 7.11, and the current profile for Case 2 is illustrated in Figure 7.4. The current speed U is given in [m/s], and current is applied in the positive x-direction. The remaining input parameters is given in Table 7.10.

Table 7.10: Input to analysis for varying current

Drag coefficient, C_D	0.7
Diameter, D	Case 3

Table 7.11: Current profiles

	U at $z = 0$	U at $z = -400$
No current	0.0	0.0
Linear current	0.8	0.0
Uniform current	0.8	0.8

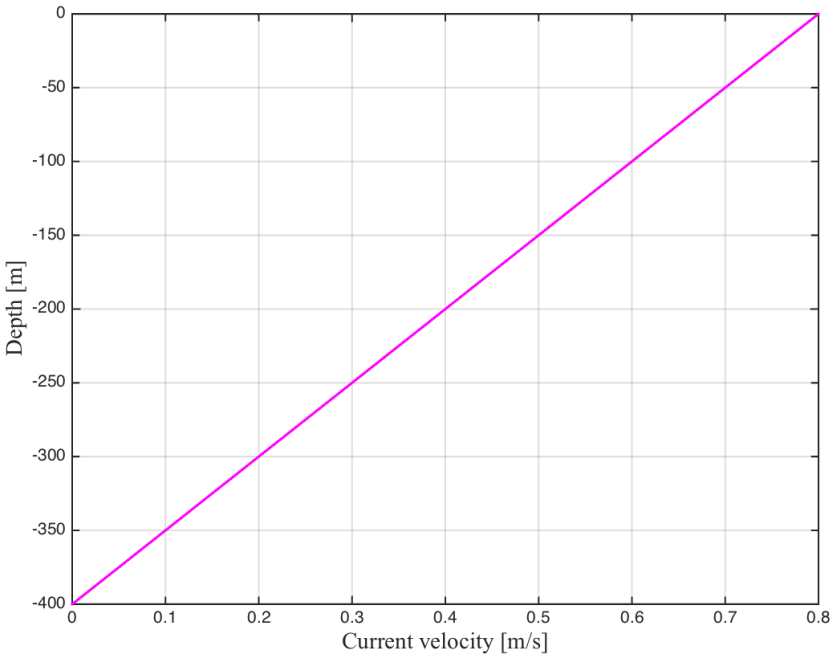

Figure 7.4: Current profile for Case 2

7.3.2 Varying Diameter

Three different diameters will be investigated here. Case 2 is adopted from the *Simple Flexible Risers*, while the values for Case 1 and Case 2 are respectively decreased and increased with 20%. The cases are presented in Table 7.13. The input of the other varying parameters, drag coefficient and current, is presented in Table 7.12.

Table 7.12: Input to analysis for varying diameter

Current, U	Uniform
Drag coefficient, C_D	0.7

Table 7.13: Diameter cases

	Outer diameter D	D [cm]	**Inner diameter** d [cm]	**Weight** [kg/m]
Case 1	8”	20.32	8	80
Case 2	10”	25.4	10	100
Case 3	12”	30.48	12	120

7.3.3 Varying Drag Coefficient

The drag coefficient C_D is defined as the non-dimensional drag-force, expressed by the term in Equation (7.7) (DNV (2010d)). Sima and RIFLEX operates in the time domain, and quadratic drag is hence utilized as explained in Section 5.2.1 on page 57. Results for varying drag coefficient is not considered in the static analysis results, as drag is a dynamic effect.

$$C_D = \frac{F_{drag}}{\frac{1}{2}\rho D u^2} \tag{7.7}$$

The input of the other varying parameters, drag coefficient and current, is presented in Table 7.14. The drag coefficient is the same for all sections of the riser (buoyancy section and regular riser section), and the cases are presented in Table 7.15.

Table 7.14: Input to analysis for varying drag, the diameter cases are presented in Section 7.3.2

Current U	Unifrom
Diameter D	Case 3

Table 7.15: Drag coefficient cases

	Drag coefficient [-]
Case 1	0.5
Case 2	0.6
Case 3	0.7
Case 4	0.8
Case 5	0.9
Case 6	1.0

7.4 Subsequent Analysis Regarding Horizontal Offset

As the last stage of the investigation of the riser response, an analysis for varying vessel positions was performed. This is an interesting parameter as it affects the tension and the curvature of the riser line. These are important parameters, and the results from this analysis can be relevant when interpreting the other parameter variations. The input values of the remaining parameters are given in Table 7.16.

Table 7.16: Input to analysis for varying horizontal offset

Current U	Unifrom
Diameter D	Case 3
Drag coefficient, C_D	0.7

The horizontal offset is defined as a position along the x-axis, the same axis as the direction of the propagating waves and current. The different positions are given in Table 7.17.

Table 7.17: Cases for varying horizontal offset

	Horizontal offset [m]
Case 1	x=350
Case 2	x=300
Case 3	x=250
Case 4	x=200
Case 5	x=150

Chapter 8

Results

In this chapter, the results from the parameter study is presented. The results from the static analyses are found in Section 8.1, and the results from the dynamic analyses are found in Section 8.2. For the static configurations, the x- and z-axis respresent the physical x- and z-direction. For the remaining plots, the x-axis represents the total riser length, in order to see the riser behaviour along its length. The riser is 644 metres long.

8.1 Static Results from Parameter Study

In the static analysis, effective tension has been considered, as well as the static XZ-configuration of the riser. Static XZ-configutation for varying current and varying diameter can be found in Figures 8.1 and 8.3, respectively. In Figures 8.2 and 8.4, the effective tension for varying current and varying diameter is shown. The results for varying drag coefficient is not displayed here, as the drag force is a dynamic effect and the results are hence the same for all drag coefficients.

8.1.1 Varying Current

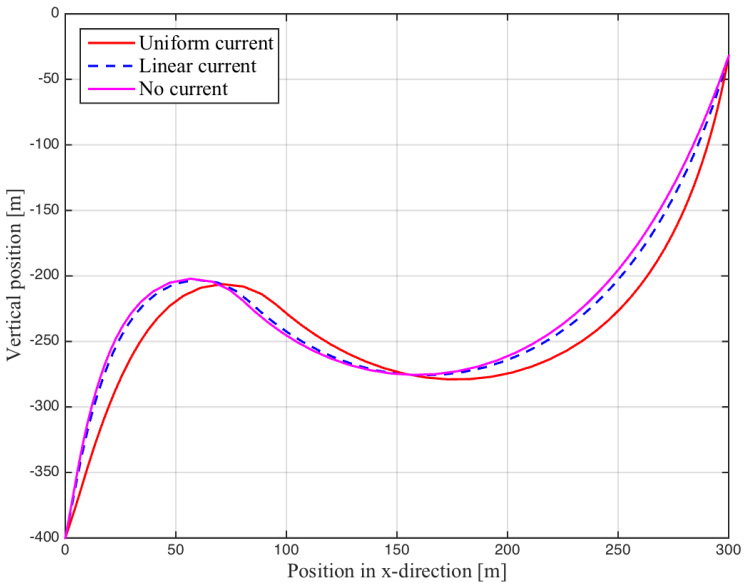

Figure 8.1: XZ-configuration for varying current

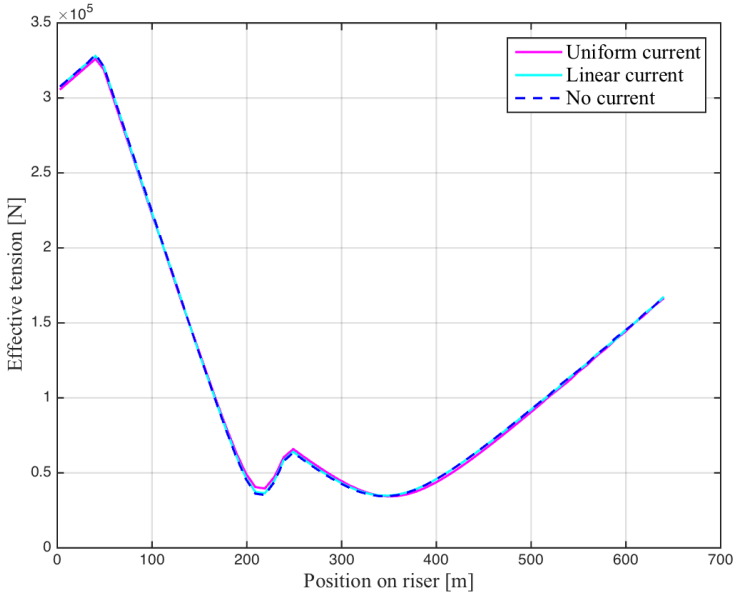

Figure 8.2: Effective tension for varying current

8.1.2 Varying Diameter

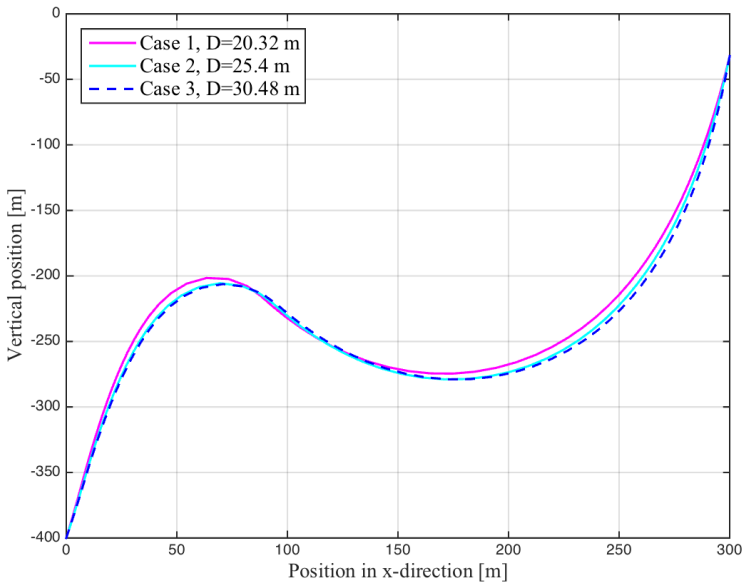

Figure 8.3: XZ-configuration for varying diameter

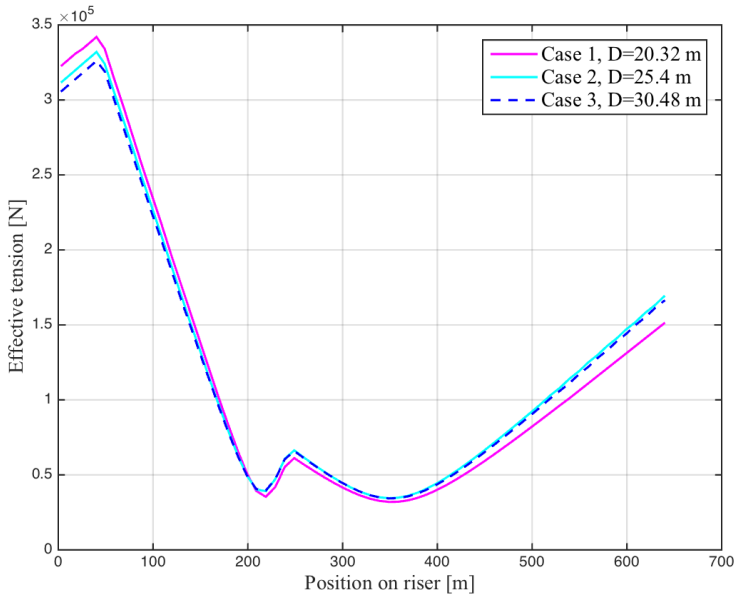

Figure 8.4: Effective tension for varying diameter

8.2 Dynamic Results from Parameter Study

In the dynamic analysis, curvature and effective tension has been considered, as well as displacements in horizontal and vertical direction. Horizontal displacement is given in x-direction, as this is the direction of the propagating waves. There is practically no displacement in y-direction. The results for varying current and varying diameter are given in Sections 8.2.1 and 8.2.2. In Section 8.2.3, the results for variation of drag are found. The plots presented can be explained as a static representation of a dynamic simulation, where the maximum and minimum values are the most extreme values that has occured during the time series.

8.2.1 Varying Current

Maximum curvature is displayed in Figure 8.5. Maximum and minimum effective tension is found in Figure 8.6. Standard deviation for effective tension is given in Figure 8.7. Horizontal and vertical displacement is given in Figures 8.8 and 8.9.

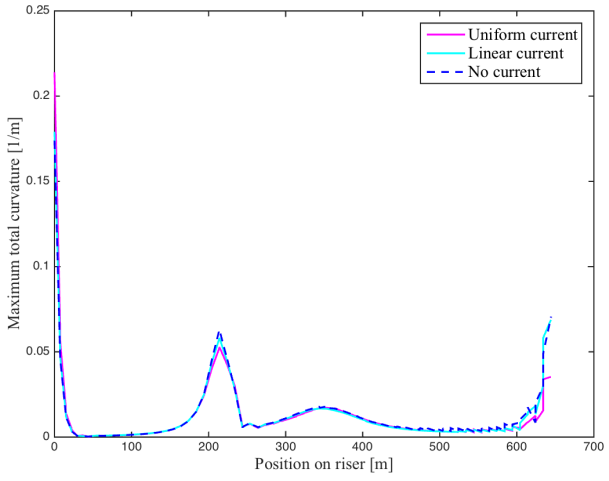

Figure 8.5: Maximum total curvature for varying current

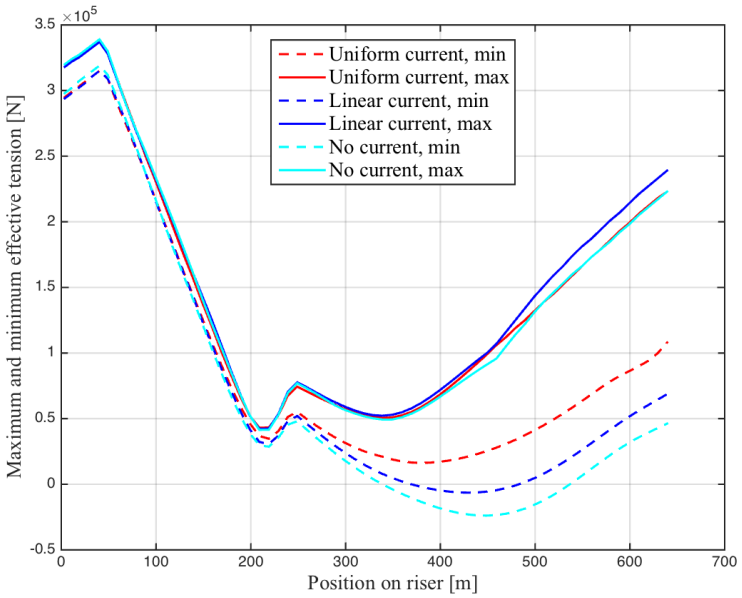

Figure 8.6: Maximum and minimum effective tension for varying current

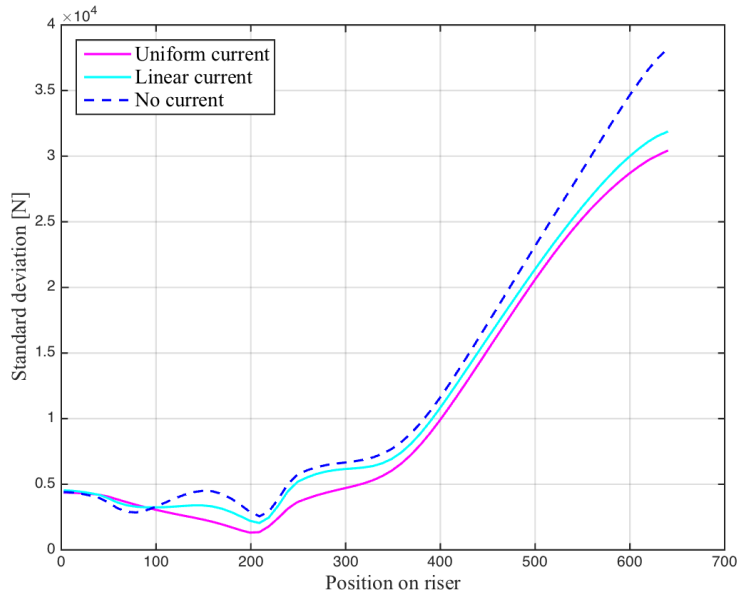

Figure 8.7: Standard deviation for effective tension, varying current

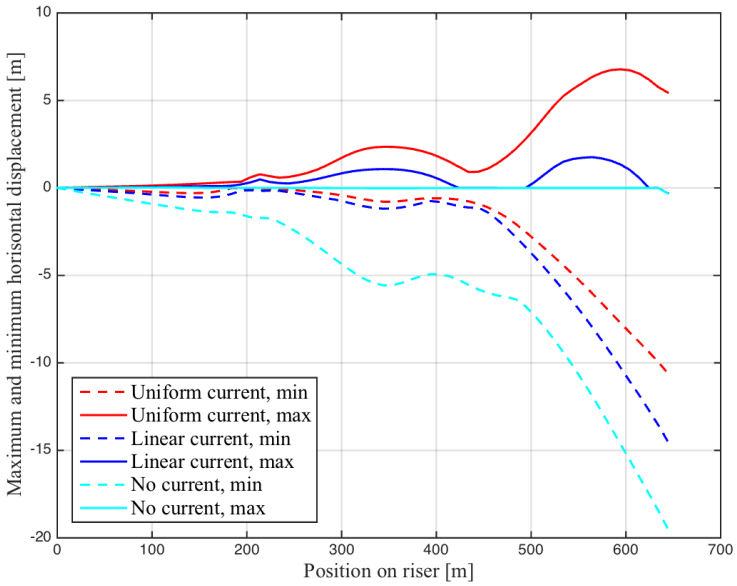

Figure 8.8: Maximum and minimum horizontal displacement for varying current

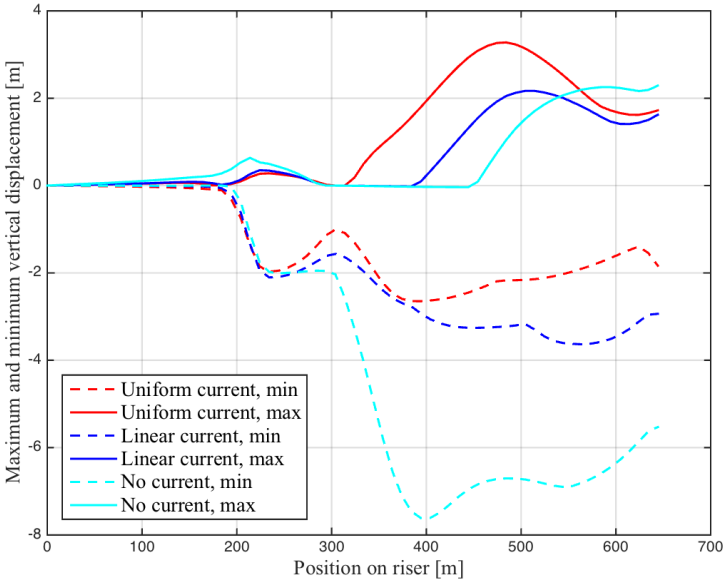

Figure 8.9: Maximum and minimum vertical displacement for varying current

8.2.2 Varying Diameter

Maximum total curvature can be seen in Figure 8.10. Figure 8.11 displays maximum and minimum effective tension. In Figure 8.12, the standard deviation for the effective tension can be seen. Horizontal and vertical displacements are given in Figures 8.13 and 8.14, respectively.

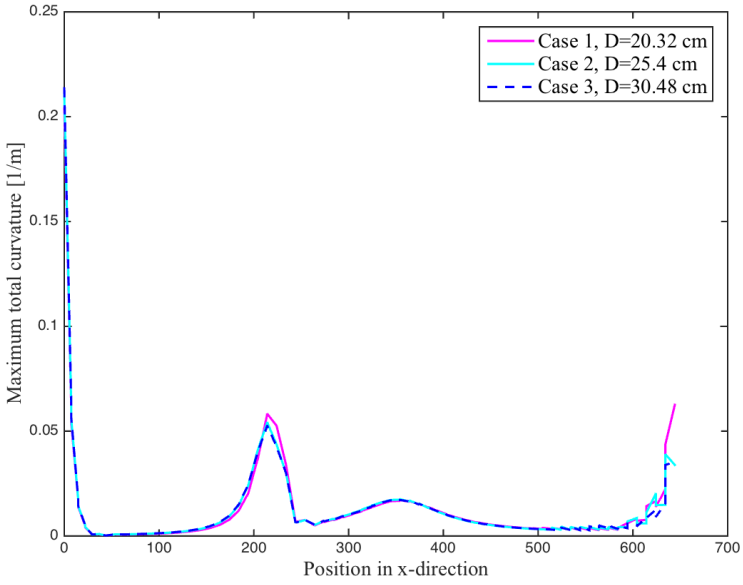

Figure 8.10: Maximum total curvature for varying diameter

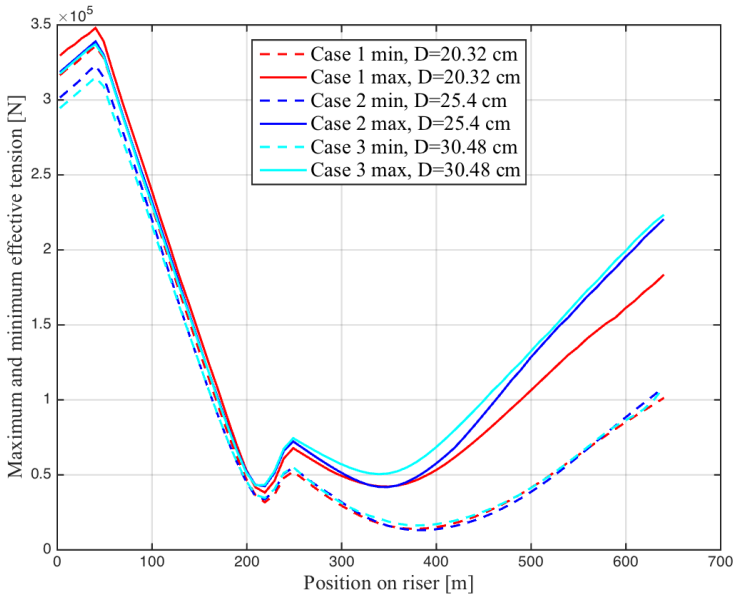

Figure 8.11: Maximum and minimum effective tension for varying diameter

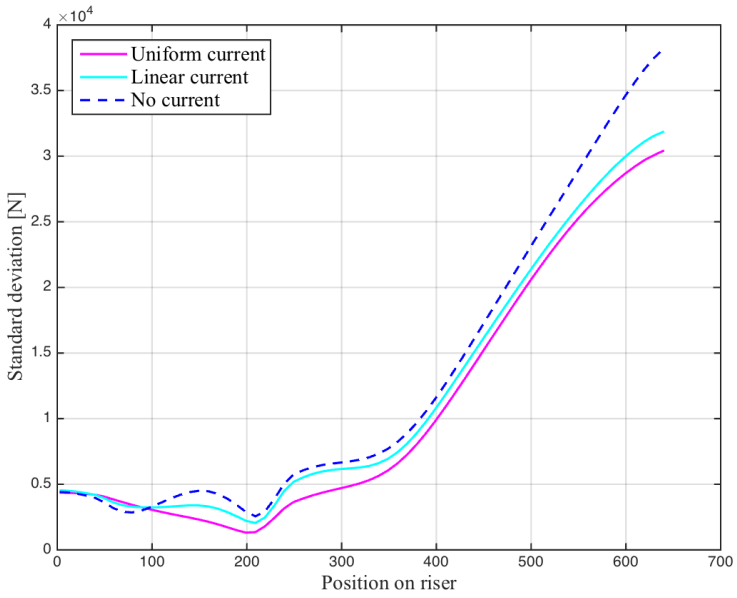

Figure 8.12: Standard deviation for effective tension, varying diameter

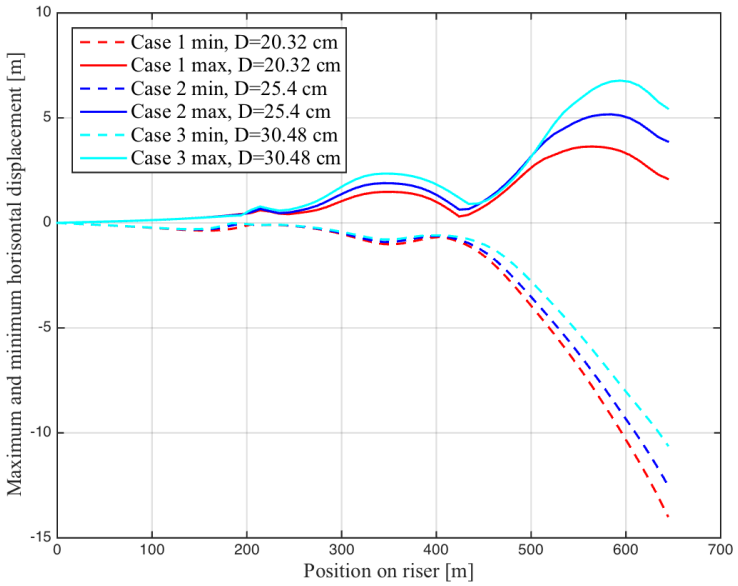

Figure 8.13: Maximum and minimum horizontal displacement for varying diameter

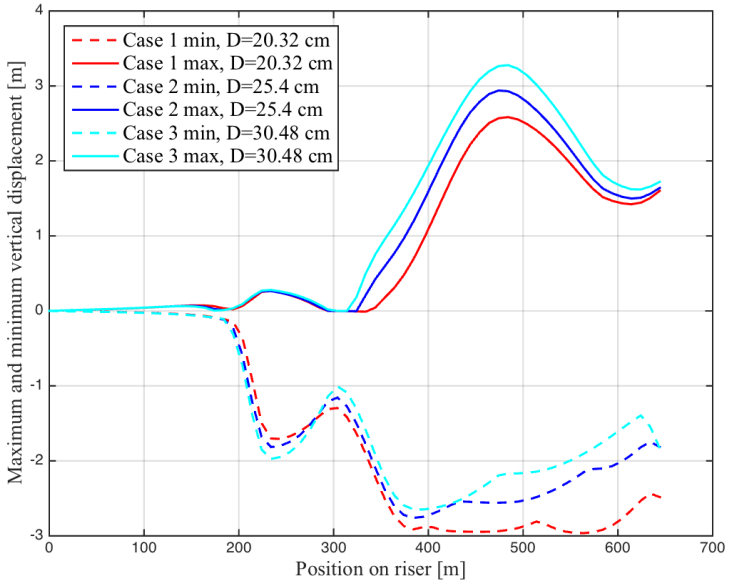

Figure 8.14: Maximum and minimum vertical displacement for varying diameter

8.2.3 Varying Drag Coefficient

The maximum total curvature can be found in Figure 8.15. Figure 8.16 displays maximum and minimum effective tension. Standard deviation for effective tension is given in Figure 8.17. Horizontal displacement is given in Figure 8.18, and the displacement in vertical direction is given in Figure 8.19.

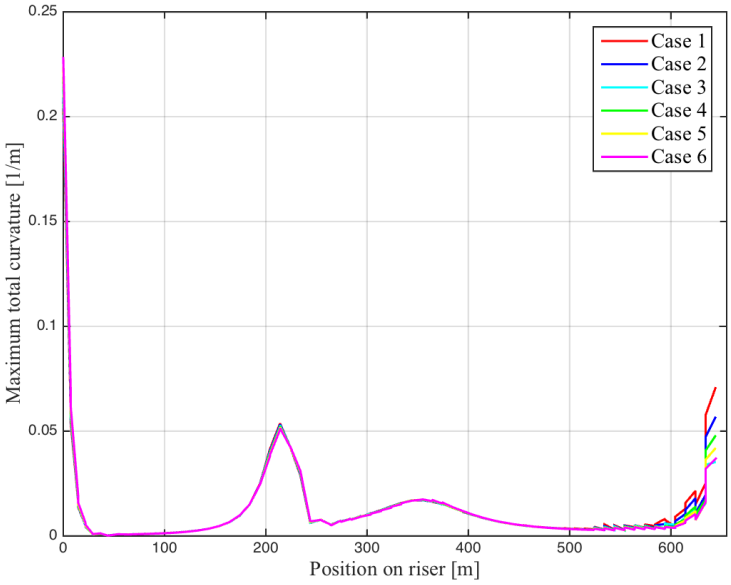

Figure 8.15: Maximum total curvature for varying drag

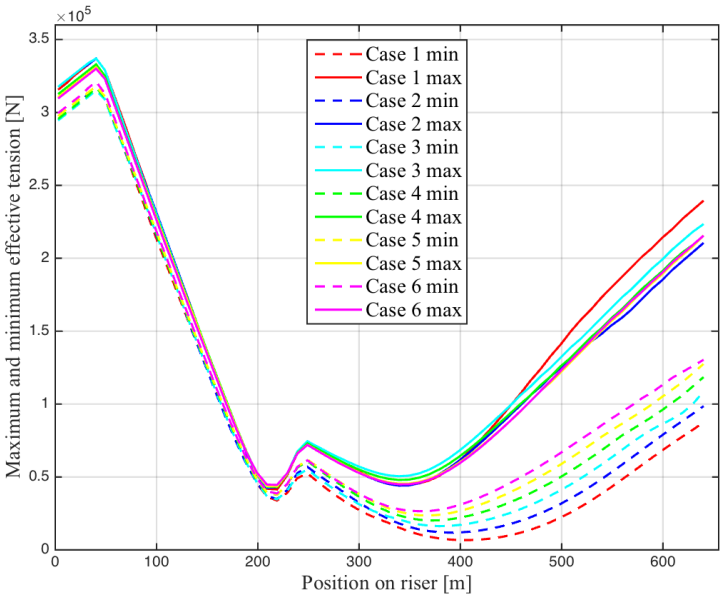

Figure 8.16: Maximum and minimum effective tension for varying drag

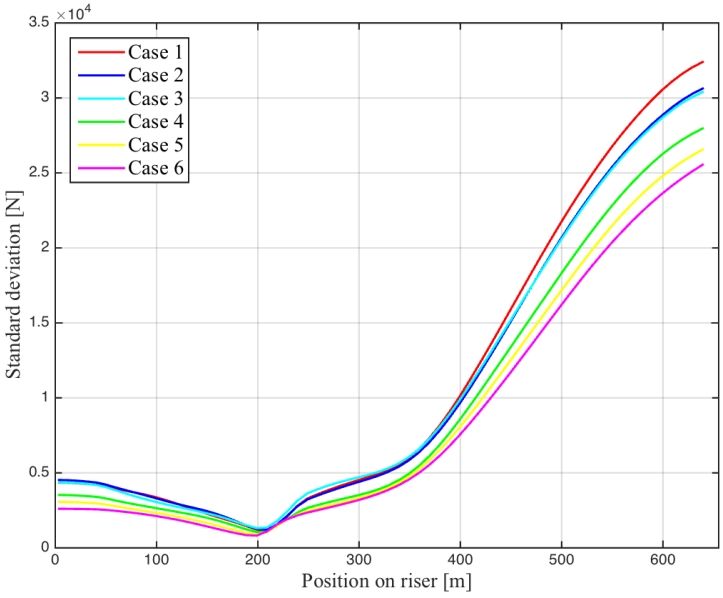

Figure 8.17: Standard deviation for effective tension, varying drag

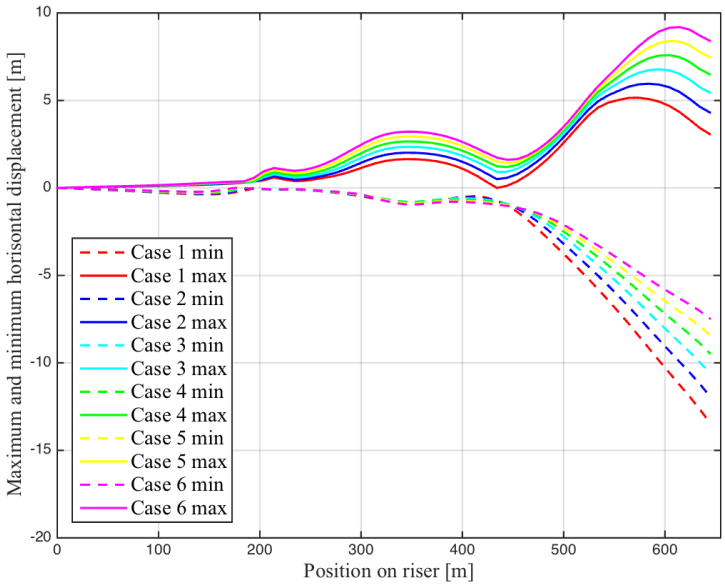

Figure 8.18: Maximum and minimum horizontal displacement for varying drag

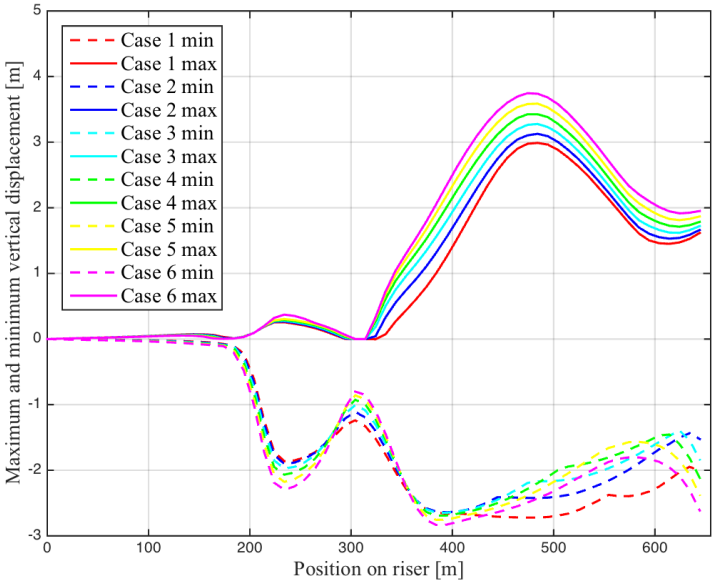

Figure 8.19: Maximum and minimum vertical displacement for varying drag

8.3 Results from Subsequent Analysis Regarding Horizontal Offset

The results from the static analysis are presented in Section 8.3.1. Figure 8.20 shows the various static configurations, and Figure 8.21 displays the static effective tension.

In Section 8.3.2, the results from the dynamic analysis can be found. The maximum total curvature can be found in Figure 8.22. Maximum and minimum effective tension is given in Figure 8.23. Standard deviation for effective tension is given in Figure 8.24. Horizontal displacement is given in Figure 8.25. The displacement in vertical direction is given in Figure 8.26.

8.3.1 Static Analysis

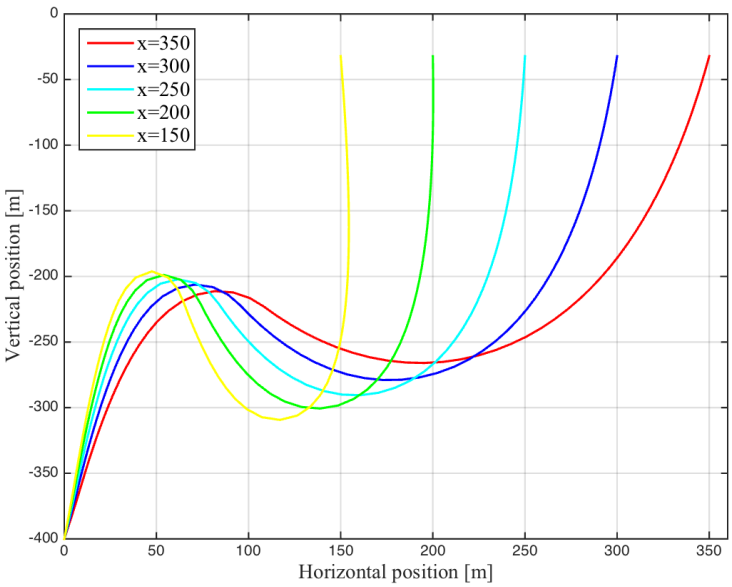

Figure 8.20: Static configuration for varying horizontal offset

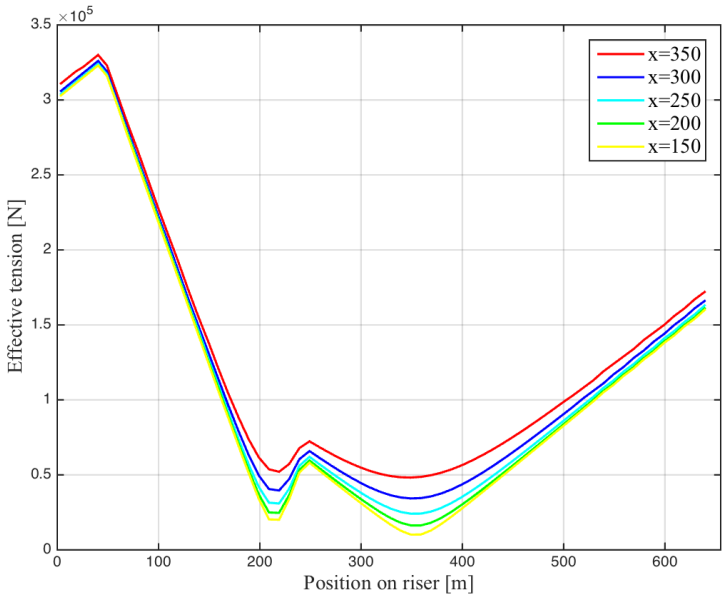

Figure 8.21: Effective tension for varying horizontal offset

8.3.2 Dynamic Analysis

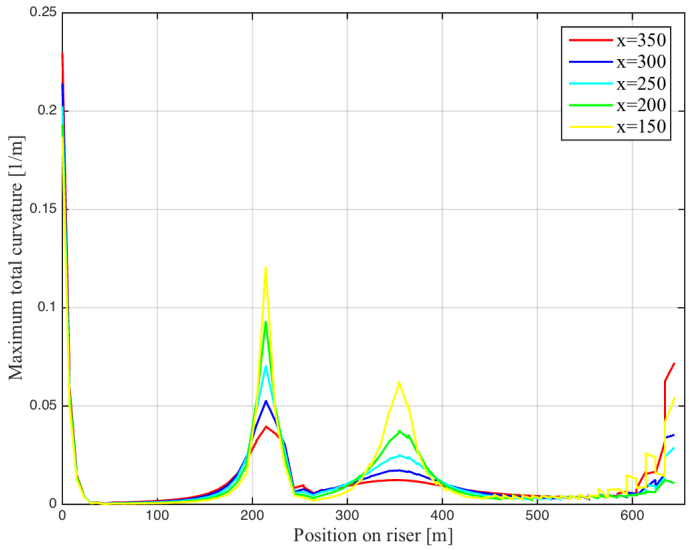

Figure 8.22: Maximum total curvature for varying horizontal offset

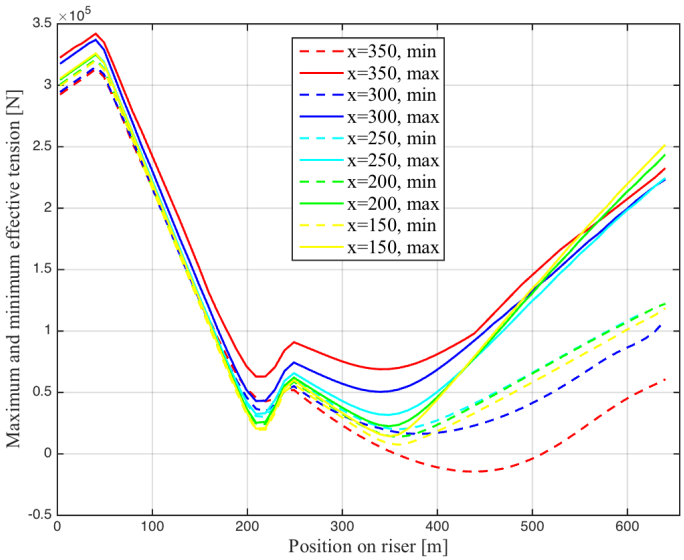

Figure 8.23: Maximum and minimum effective tension for varying horizontal offset

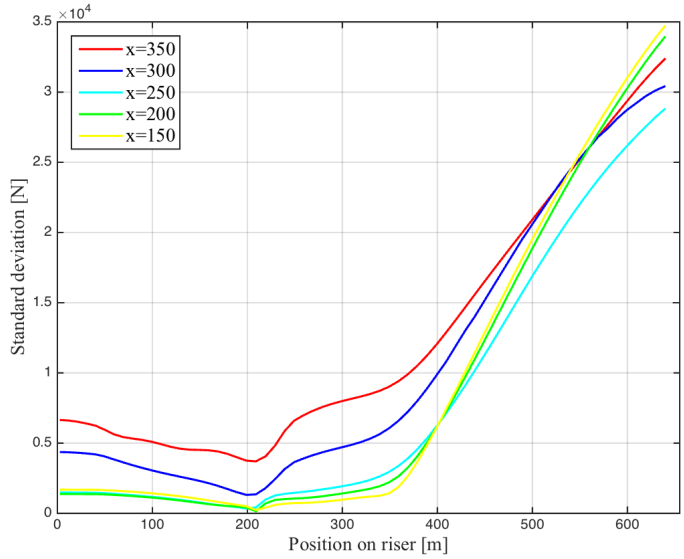

Figure 8.24: Standard deviation for effective tension, varying horizontal offset

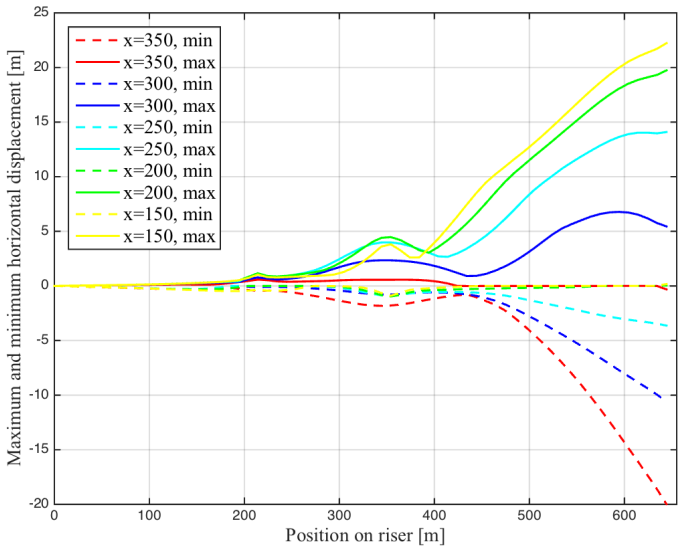

Figure 8.25: Maximum and minimum horizontal displacement for varying horizontal offset

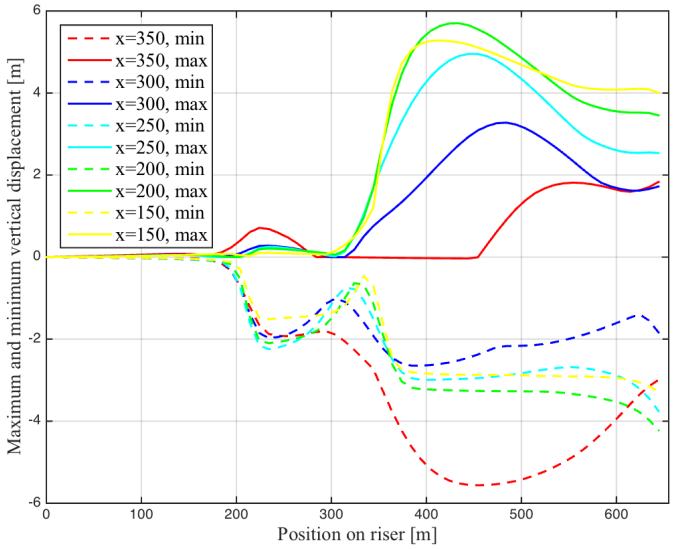

Figure 8.26: Maximum and minimum vertical displacement for varying horizontal offset

Chapter 9

Discussion

In this chapter, the results are discussed. In Section 9.1, the results for the study of varying horizontal offset are discussed. These results are presented first, even though the analysis was performed after the original parameter study. The reason for this is that these results are relevant for interpretation of some of the results in the original parameter study. The discussion of the results for varying current, diameter and drag coefficient follows in Sections 9.2, 9.3 and 9.4.

For the curvature plots, the graphs seem innacurate and discontinuous for some areas. In these cases, more detailed results should have been retrieved from the analysis by changing the time step , as there is an uncertainty in the presented results, especially towards the riser hangoff. Still, for most plots, it is possible to see trends.

9.1 Horizontal Offset

From the results of the three parameter variation, it was suspected that the initial horizontal offset of the platform influenced the results. Hence, the analysis for varying horizontal offset was executed.

The results imply that larger horizontal offsets lead to larger curvature at the riser top and at the seabed, while for small horizontal offsets, the curvature increases for the two arcs in the middle of the riser, see Figure 8.22. The same trend can be found in the plot showing the static configuration in Figure 8.20. When the horizonal offset is 250 metres, which is the midpoint of the investigated offsets, the configuration will experience some curvature at the four mentioned critical points. This configuration experiences least effective tension in the upper part of the riser, as well as having the smallest standard deviation regarding effective tension in the riser. It is important to note that this analysis is performed with a 50 metre interval between the offsets, and hence will the position with minimum tension forces not be exactly at $x = 250$ [m], but it has the lowest tension out of the investigated positions. This configuration is further referred to as MFC (minimum force configuration).

In a real situation, when choosing the platform position, MFC would not necessarily be the desired configuration. Many factors need to be considered. For instance, higher tension reduces the possibilities for movement, which in many cases is desirable. MFC has a larger heave response than the configuration used for the parameter study in this task, $x = 300$ [m]. This can be seen in Figure 8.26, which shows vertical displacement.

When considering the horizontal displacement of the riser top, it is seen that for the largest horizontal offset, the riser moves only in the negative x-direction, while

for the small offsets, the only movment is in the positive x-direction from initial position. This could imply that the riser seek to obtain a position nearer to MFC. It is important to note that the vessel motion will be governing, not the motion of risers. In these analysis results, it may seem as if the riser properties decide the motions. This behaviour is probably due to choice of boundary conditions.

In hindsight, it could have been desirable to perform the parameter study at MFC, as this would lead to a lower top tension in the riser as a starting point, and the response due to other parameter changes would be easier to detect.

9.2 Varying Current

For varying current, the static configuration in Figure 8.1 shows a large difference for the uniform current compared to the cases with linear current and no current. The current close to the seabed seems to have a great impact on the horizontal displacement of the riser. The riser is shifted considerably in positive x-direction. For the linear current, the same trend is seen compared to no current, but the change in horizontal position is mainly noticable closer to the sea surface, and the displacement is much smaller. This shows that a current with high velocity for large depths will influence sufficiently more, also towards the top, than current that mainly affects the riser near the top.

From the dynamic analysis, it can be seen in Figure 8.5 that the maximum curvature near the surface is smallest for the case with uniform current, while the the other two cases are nearly similar. This reflects what can be seen from the static configurations.

Regarding effective tension, it can be seen that the case with the linear current obtains the largest effective tension in the upper part of the riser. The reason for this

might be that both the waves and the current act on the upper part of riser, while further down, both these effect cease. This creates a difference in how the riser is affected by loading over the length. The two other cases have approximately equal maximum effective tension, but the standard deviation is largest for the case with no current and smallest for the case with uniform current. This is probably due to the wave particles going in both positive and negative x-direction, and the current moves constantly in positive x-direction. At the riser top in the plot in Figure 8.7, this is seen most clearly, as the case with no current has a significantly larger standard deviation. The waves are allowed to act more on the riser in this case as there is no counter effect to the waves.

For the case with no current, the results show that the riser never moves on postive x-direction from initial position, i.e. it moves only in opposite direction as the propagating waves. For both cases with present current, there are displacements in the direction of the propagating waves and current, larger such for the uniform current. Still, the displacements in negative x-direction are large. It may again seem as if the riser behaves to obtain a position closer to MFC. These results were part of the reason why the horizontal offset was investigated further. The horizontal displacements for varying current indicates that the boundary conditions could have been chosen differently. Horizontal displacements of this magnitude are unlikely to occur physically, as the floater mass will be too large. The floater movement will be governing for the system response, and the external loading will most likely not affect the horizontal displacement to this extent.

For increasing current, the riser starts to displace vertically from initial position at a point further down in the riser column. The total deviation from initial position is largest for the case with no current, and at the riser top, this also has the largest displacement in positive z-direction. One explanation for this could be that cur-

rent also creates a damping, and it is possible that this happens here. If the damping counteracts the vessel heave motion, the results correspond to this.

9.3 Varying Diameter

When discussing the results from the analysis with varying diameter, it is important to note that the weight has been changed as well. The additional buoyancy obtained by increase of volume, does not even out the additional weight . This can be seen in the static configuration of the system in Figure 8.3, where the riser hangs lower in the water for increasing diameter and weight. This means that the weight increase may effect the results more than the change in diameter. The results are discussed based on this notion.

In the upper part of the riser, increasing diameter results in increasing values for maximum effective tension. Minimum effective tension is not largely affected by the variation. At the riser top, the smallest diameter have lowest effective tension force, while the two larger diameters result in an almost equal effective tension. The drag term in Morison's equation is dependent on the diameter, and the inertia term is dependent on the diameter squared. According to this, an increase in diameter will largely increase the forces, but again, so will the increased weight. The riser motion will also affect the forces in the riser column.

When looking at the plot for standard deviation in Figure 8.12, it can be seen that the standard deviation is increasing for increasing diameter. This may be as the larger diameters result in a larger area for the forces to attack, and the effect is larger. In this case, increased mass will contribute with additional inertia, but it is hard to determine the importance of this in comparance.

The curvature at the top decreases for increasing riser diameter and weight, as these will hang more vertically down from the hangoff point. The same trend can be seen around the buoyancy section, where the riser with lower weight is lifted up higher in the water.

Both the horizontal and vertical displacement behaviour follows a similar trend for all three diameters, see Figures 8.13 and 8.14, but the results show that for increasing diameter, the displacement interval lies further in the positive x-direction, and the vertical displacement interval lies nearer the sea surface. An explanation of this behaviour can be that the water particles of the wave are acting in a circular direction, this alternating between amplifying and reducing the effect of the current. This will affect the top of the riser, while further down, the effect of the waves is smaller. The riser motion due to this effect will cause these displacements, ref. Morison's equation with relative velocity given in Equation (5.3) on page 56.

When comparing to the horizontal offset variation, the configurations with less curvature at the top tend to have a response in vertical direction nearer the sea surface, see Figure 8.26. The same trend is seen here.

9.4 Varying Drag Coefficient

For increasing drag coefficients, the curvature seems to decrease at the riser top. At the seabed, the curvature seems to be unchanged. This is due to more motion closer to sea surface, and hence a larger drag force. This is shown in the Figures 8.15.

For minimum and maximum effective tension shown in Figure 8.16, the trends are not as apparent. The minimum force increases for increasing drag, as would be expected. For the maximum tension, there is no obvious trend or systematic

response. For Case 1, with the smallest drag coefficient, the riser expereinces the largest maximum effective tension. For Case 2, the lowest value for maximum effective tension is obtained. For the remaining cases, with larger drag coefficients, the graphs representing the maximum tension are located in between the two first graphs. The reason for this behaviour is not detected. One possible explanation is that drag foces can act both as excitation and damping, as described in Section 5.2.1 og page 57, and that this is an influencing factor that affects the results.

The results for the standard deviation are more systematical. As drag forces act in the opposite direction of the fluid, increasing drag coefficient results in smaller amplitude response of the riser, see Figure 8.17.

For the displacements, the response for increasing drag coefficient shows the same trends as for increasing diameter. The displacement for the different drag coefficients follow approximately the same movement pattern. Increasing values of C_D lead to horizontal displacement in increasing positive the x-direction, as displayed in Figure 8.18, and for the vertical displacement interval to be nearer the surface. The same proposed explanation can be used here as for the case with varying diameter; the wave particle moves in a circular motion, and the riser is more affected by the waves at the upper parts. The riser obtains a motion near the top, and this motion is origin to the displacement patterns. Near the riser hangoff, there is very little variation in the displacement in the z-direction, but til is can be explained from it being the riser properties that have changed, and that the vessel is not affected by this. Further down on the riser, the riser properties are more prominent, and it can displace from initial position.

9.5 Sources of Error

- The bilge box on the Goliat FPSO was ignored. If this was included, a different motion pattern would be obtained. Hence, the RAO-file imported into RIFLEX, and again the riser response, would be different.
- General simplifications in model. For instance, COG is calculated based on assumptions. This will affect the characteristic motion of the FPSO.
- Boundary conditions are important in structural analyses, and the choice of these is crucial regarding the riser response. In the dynamic analyses, the riser deflects in x-direction, in a way that could imply that it is able to move away from the platform. This seems not to be the case in z-direction.
- The weight is varied too much with varying diameter, which might lead to some results being more affected by the weight change, rather than the diameter change.
- The riser wall thickness has not been considered in the analysis. The inital riser cross-section was adopted from the RIFLEX task used as a starting point for the riser model. These values might not be realistic.
- There are always some unceratinties present when using software analysis tools, and errors might occur as a result of this. This could be user errors, computational errors or regarding the software sensitvity.

Chapter 10

Conclusion and Suggestion to Further Work

10.1 Conclusion

In this thesis, analyses for varying parameters are performed. In the original parameter study, current, diameter and drag coefficient were subject to change. Subsequently, an analysis regarding horizontal offset was performed, where the results showed that, out of the investigated positions, a horizontal offset at 250 metres relative to TDP would give least effective tension in the riser. This configuration is referred to as MFC. The parameter study was perfomred for a horizontal offset of 300 metres, and it is suggested that the MFC position would be a more optimal offset for the parameter study, as less tension would allow more motion, and effects of parameter variation would be more visible.

For increasing current, the riser is shifted in the positive x-direction, and the curvature at the top decreases. The linear current profile obtains the largest effective tension

in the upper section of the riser. The cases for uniform current and no current are much the same regarding maximum effective tension, but the case with no current has a larger response amplitude.

For the study of varying diameter, the weight was changed too much relative to diameter. This may result in weight change being governing, rather than the diameter change, for some of the effects seen in the results. For instance, the static configuration implies this, as the risers with larger diameter and weight hangs lower in the water. Regarding tension and curvature, the two risers with largest diameters and weight behave similarly, compared to the smallest riser. The two largest have less curvature at the hangoff, and experience larger tension.

For changing diameter and drag, the vertical displacement at the riser top is just merley influenced. This could be due to the riser properties being altered, and not the environment. For changing riser properties, the platform behaviour hardly change. Contrary, for varying current, a distinguishable variation is seen in the vertical direction. This may be as the current will have an impact on the vessel motion, and hence the riser top's position in z-direction.

Even though the top of the riser, i.e. the vessel motion, is affected only to a small extent regarding vertical displacement, the riser shows varying behaviour further down and towards the middle of the riser. For increasing diameter and drag coefficients, the vertical displacements are shifted closer to the sea surface. The horizontal displacements are shifted in the positive x-direction. By increase of the drag-coefficient, the curvature at the riser hangoff decreases.

10.2 Suggestions to Further Work

- Investigate the effect of weight change compared to the effect of diameter change. Changing only the diameter, or changing the two parameters with correct ratio, is desired. A comparison with existing result should be performed.
- Create a more detailed version the Goliat FPSO. Firstly, an inclusion of the bilge box is likely to influence the motion pattern significantly. Further, with access to more detailed vessel specifics, the actual COG could be applied to the mass model.
- Importing the model into Sima, to create a coupled SIMO/RIFLEX task. This way, the riser response could be investigated in context with the vessel response.
- Further investigation of effective tension due to variation of the drag coefficient, as the results did not show systematic behaviour.
- More sensitivity studies should be performed regarding the vessel and riser setup, particularly the boundary conditions.
- A parameter study regarding wall thickness should be performed.
- Standard deviations should be investigated for all dynamic results.

References

Aker Engineering & Technology (Ed.). (2015). *Floating production storage and offloading (FPSO).* Retrieved from http://www.akersolutions.com/en/Global-menu/Products-and-Services/Engineering/Floater-designs/Floating-production-storage-and-offloading-FPSO/

Alfieri, M. (2016). *Goliat the giant.* Retrieved from www.eniday.com/en/technology_en/goliat-norway-offshore-oil-production

Amdahl, J., Endal, A., Fuglerud, G., Hultgreen, L. R., Minsaas, K., Rasmussen, M., ... Valland, H. (2011). *Kompendium i marin teknikk intro og marin teknikk 1.*

API. (2002). API Recommended Practice 17B. *Recommended Practice for Flexible Pipes.*

API (Ed.). (2015). *Offshore Access to Oil and Natural Gas Resources.* Retrieved from http://www.api.org/oil-and-natural-gas-overview/exploration-and-production/offshore/offshore_access_to_americas_resources

Bjorneseth, D. M., F.B. & Strand, J. (2008). Dynamic positioning system-usability and interaction. In ACM (Ed.), *Proceedings of nordichi.*

BW Offshore (Ed.). (2015). *Learn more about the fpso.* Retrieved from http://www.bwoffshore.com/business/technicals/

de Camargo, F. V., Guilherme, C. E. M., Fragassa, C. & Pavlovic, A. (2016). Cyclic

stress analysis of polyester, aramid, polyethylene and liquid crystal polymer yarns.

De-icing a cargo boat. (2010). Retrieved from https://www.groupocean.com/en/achievements/view/21

DNV. (2009). Offshore Standard - Steel Wire Ropes. *DNV-OS-E304*.

DNV. (2010a). Composite Risers. *DNV-RP-F202*.

DNV. (2010b). Environmental Conditions and Environmental Loads. *DNV-RP-C205*.

DNV. (2010c). Global Performance Analysis of Deepwater Floating Structures. *DNV-RP-F205*.

DNV. (2010d). Modelling and analysis of marine operations. *DNV-RP-H103*.

DNV. (2010e). Offshore Standard - Dynamic Risers. *DNV-OS-F201*.

DNV. (2010f). Offshore Standard - Position Mooring. *DNV-OS-E301*.

DNV (Ed.). (2011). Sesam user manual - genie vol. 1 [Computer software manual].

DNV-GL (Ed.). (2013). *Sesam hydrod - advanced stability and hydrodynamic analysis made easy.*

DNV-GL (Ed.). (2016). *Frequency domain hydrodynamic analysis of stationary vessels - wadam.* Retrieved from https://www.dnvgl.com/services/frequency-domain-hydrodynamic-analysis-of-stationary-vessels-wadam-2412

ENI (Ed.). (2011). *Wind and weather in the barents sea.* Retrieved from http://oljevern.no/en/page/?nr=19

ENI (Ed.). (2015). *Facts.* Retrieved from http://www.eninorge.com/en/field-development/goliat/facts/

ENI (Ed.). (2016a). *Goliat i produksjon.* Retrieved from http://www.eninorge.com/no/Feltutbygging/Goliat/

ENI (Ed.). (2016b). *Goliat platform now in hammerfest.* Retrieved from

http://www.eninorge.com/en/News--Media/News-Archive/2015/-Goliat-platform-now-in-Hammerfest/

Faltinsen, O. (1990). *Sea Loads on Ships and Offshore Structures*.

GATE (Ed.). (2015). *Introduction to risers*. Retrieved from http://www.gateinc.com/gatekeeper/gat2004-gkp-2015-02

Greco, M. (2012). *Tmr4215: Sea loads. lecture notes*.

Gundersen, P. (2012). Methodology for determining remnant fatigue life of flexible risers subjected to slugging and irregular waves. In ASME (Ed.), *Omae2012*.

Heidrun. (2015). Retrieved from http://www.norskolje.museum.no/en/heidrun-3/

Holm, M. (Ed.). (2016a). *Feltdata - Goliat*. Retrieved from http://offshore.no/feltdata?navn=GOLIAT

Holm, M. (Ed.). (2016b). *Feltdata - Heidrun*. Retrieved from http://offshore.no/feltdata?navn=HEIDRUN

Holm, M. (Ed.). (2016c). *Feltdata - Snorre*. Retrieved from http://offshore.no/feltdata?navn=SNORRE

Iden, K. A., Reistad, M., Aarnes, O. J., Gangstø, R., Noer, G. & Hughes, N. E. (2012). *Kunnskap om vind, bølger, temperatur, isutbredelse, siktforhold mv. - "barentshavet sØ"* [Environmental impact assessment].

Larsen, C. M. (2015). *TIM4182 - Marine Dynamics*.

Major, F. (2013). *Benefits of a cylindrically shaped floater for an FPSO application in cyclone exposed environments* [Presentation]. INTSOK Deep Water Conference. Retrieved from http://www.norwep.com/content/download/20450/128357/version/2/file/01_Sevan_Fredrik+Major.pdf

Marintek (Ed.). (2011). RIFLEX User Manual [Computer software manual]. MARINTEK.

Marintek (Ed.). (2015). RIFLEX Theory Manual [Computer software manual].

MARINTEK.

Mazzetti, M. J. (2015). *Restvarme fra plattformer krymper utslipp.* Retrieved from http://petro.no/restvarme-fra-plattformer-krymper-utslipp/26695

McCaul, J. R. (2001). Deepwater remote fields rely on floating production systems.

NGI (Ed.). (2011). *Torpedo anchors.* Retrieved from http://www.ngi.no/ngi/pdf/ProductSheet.aspx?id=31988&mode=view&epslanguage=NO

Nielsen, F. G. (2007). *Lecture notes in marine operations.*

NSIDC (Ed.). (2016). *Quick facts on icebergs.* Retrieved from https://nsidc.org/cryosphere/quickfacts/icebergs.html

NTNU (Ed.). (2015). *Drag forces in dynamic analysis.*

Oil and Gas People (Ed.). (2016). *Aker solutions wins trestakk topside feed, tie-in to Åsgard a.* Retrieved from https://www.oilandgaspeople.com/news/6945/aker-solutions-wins-trestakk-topside-feed-tie-in-to-asgard-a/

OTC (Ed.). (1995). *Dp assisted and passive mooring for fpsos.*

OTC (Ed.). (2001). *Fpso design and conversion: A designer's approach.*

Palmer, A. & Croasdale, K. (2012). *Arctic offshore engineering.*

Pettersen, B. (2007). *Marin teknikk 3, hydrodynamikk.*

PR Newswire (Ed.). (2013). Eni norge to manage engineering data with intergraph solutions in the climate-challenging conditions of the barents sea goliat field.

PSA (Ed.). (2014a). *Facts about the far north.* Retrieved from http://www.psa.no/facts-the-far-north/cold-article10447-1143.html

PSA (Ed.). (2014b). *Facts about the far north.* Retrieved from http://www.psa.no/facts-the-far-north/ice-article10448-1143.html

PSA (Ed.). (2014c). *Facts about the far north.* Retrieved from http://www.psa

.no/facts-the-far-north/darkness-article10449-1143.html

PSA (Ed.). (2014d). *Facts about the far north.* Retrieved from http://www.psa.no/facts-the-far-north/cold-article10447-1143.html

PSA (Ed.). (2014e). *Facts about the far north.* Retrieved from http://www.psa.no/facts-the-far-north/distance-article10444-1143.html

Ree, M. (2013). *Aasta hansteen: Krevende, dyrt og usikkert.* Retrieved from https://www.tu.no/artikler/aasta-hansteen-krevende-dyrt-og-usikkert/275351

Rigzone (Ed.). (2015a). *How do fpsos work?* Retrieved from http://www.rigzone.com/training/insight.asp?insight_id=299

Rigzone (Ed.). (2015b). *How do mooring systems work?* Retrieved from http://www.rigzone.com/training/insight.asp?insight_id=358&c_id=17

Rigzone (Ed.). (2015c). *How do semisubmersibles work?* Retrieved from http://www.rigzone.com/training/insight.asp?insight_id=338

Rigzone (Ed.). (2015d). *How do spars work?* Retrieved from http://www.rigzone.com/training/insight.asp?insight_id=307&c_id=12

Sevan Marine (Ed.). (2016). *Sevan 1000 fpso for goliat.* Retrieved from http://www.sevanmarine.com/component/content/article?id=582:sevan-1000-fpso-for-goliat

SINTEF. (n.d.). *Handbook on design and operation of flexible pipes.*

Statoil (Ed.). (n.d.-a). *Heidrun.* Retrieved from https://www.statoil.com/en/what-we-do/norwegian-continental-shelf-platforms/heidrun.html

Statoil (Ed.). (n.d.-b). *Snorre.* Retrieved from https://www.statoil.com/en/what-we-do/norwegian-continental-shelf-platforms/snorre.html

Statoil (Ed.). (n.d.-c). *Åsgard.* Retrieved from https://www

.statoil.com/content/statoil/no/what-we-do/norwegian
-continental-shelf-platforms/asgard.html?gclid=
Cj0KEQiA88TFBRDYrOPKuvfY2pIBEiQA97Z8MRtOB7YcM89nM5FMsmolKgbdm2jPsv59xlq7aqu7bV

Stensvold, T. (2014). *Det meste er ekstremt på Aasta Hansteen.* Retrieved from https://www.tu.no/artikler/industri-det-meste-er-ekstremt-pa-aasta-hansteen/231120

SubseaIQ (Ed.). (2015). *Goliat.* Retrieved from http://subseaiq.com/data/Project.aspx?project_id=400&AspxAutoDetectCookieSupport=1

Sævik, S. (2015). *Lecture notes in offshore pipeline technology.*

Torpedo anchor. (2015). Retrieved from http://coolarcticmoorings.weebly.com/uploads/1/0/3/4/10343992/298554512.jpg

Witz, J. A. (1996). A case study in the cross-section analysis of flexible riser.

Appendices

Appendix A

Riser data

Parameter	Value	Unit
Axial stiffness	$1 \cdot 10^9$	[N]
Bending stiffness	$1 \cdot 10^4$	[Nm^2]
Torsion stiffness	$1 \cdot 10^5$	[Nm^2/rad]
Tension capacity	$1 \cdot 10^9$	[N]
Max curvature	0.4	[1/m]
Density of internal fluid	1000	[kg/m^3]

Appendix B

Location parameters

Parameter	Value	Unit
Gravity	9.81	[m/s^2]
Air density	1.3	[kg/m^3]
Kinematic viscosity of air	$1.824 \cdot 10^{-5}$	[m^2/s]
Water density	1025	[kg/m^3]
Kinematic viscosity of water	$1.88 \cdot 10^{-6}$	[m^2/s]